 CMC, vol.39, no.3, pp.231-265, 2014

Effective Surface Susceptibility Models for Periodic Metafilms Within the Dipole Approximation Technique

A.I. Dimitriadis[1], **N.V. Kantartzis**[1] **and T.D. Tsiboukis**[1]

Abstract: The most important surface susceptibility models for the electromagnetic characterization of periodic metafilms, based on the dipole approximation method, are systematically analyzed in this paper. Specifically, two well-known techniques, which lead to a set of local effective surface parameters, are investigated along with a new dynamic non-local modeling algorithm. The latter formulation is properly expanded, in order to be applicable for any arbitrary periodic metafilm, irrespective of its way of excitation. The featured schemes are then directly compared toward their ability to efficiently predict the reflection and transmission properties of several lossless and lossy metafilms. Their outcomes are carefully verified through an assortment of numerical simulations, while novel physical insights of the observed phenomena and diverse implementation aspects of the models are extensively discussed.

Keywords: Bianisotropic scatterers, electromagnetic characterization, metafilm, non-local effective parameters, particle polarizabilities, surface susceptibilities.

1 Introduction

Since the first experimental demonstration and subsequent exploding development of double-negative (DNG) metamaterials after the year 2000, one of the most significant challenges that occurred has been the push of artificial magnetic properties toward optical frequencies. To this end, a large number of homogenization methods has been suggested, in order to validate the effective magnetic response of such artificial structures. However, despite the multitude of successive efforts that have been published in the literature, a unified approach for the unambiguous effective-medium representation of all bulk metamaterials is yet to be developed.

In the meanwhile, the 2-D equivalents of bulk metamaterials, frequently designated as metafilms, have also been heavily analyzed. These structures are typically

[1] Aristotle University of Thessaloniki, GR-54124 Thessaloniki, Greece.

formed by the 2-D periodic repetition of non-intersecting, properly-engineered scatterers or meta-atoms. Initially, their theoretical treatment has been, in essence, identical to that of their 3-D counterparts, thus leading to the assignment of bulk effective constitutive parameters ε_{eff} and μ_{eff}. Later, the authors of [Holloway, Dienstfrey, Kuester, O'Hara, Azad and Taylor (2009)] have proven the inconsistency of such procedures, as for realistic metafilms (when the thickness of the structure along the direction normal to the periodicity is $d \ll \lambda$), the values of ε_{eff} and μ_{eff} depend on thickness d. Since d cannot be uniquely defined, due to the lack of periodicity along this direction, the corresponding bulk effective constitutive parameters do not have their usual physical meaning and cannot be considered as characteristic parameters of the structure under study.

A viable alternative for the electromagnetic characterization of metafilms is the extraction of appropriate boundary conditions, which efficiently correlate the electromagnetic fields on the two sides of the metafilm to a macroscopic average of its actual micro-structure. These macroscopic parameters are called effective surface susceptibilities and represent the surface equivalent of ε_{eff} and μ_{eff} bulk constitutive parameters. Nonetheless, contrary to them, surface susceptibilities can be unambiguously attributed to a metafilm and hence, they constitute a sufficient set of parameters for its description. In fact, once these parameters are known or can be calculated, an effective-medium representation of the metafilm is achieved and boundary conditions are only needed to compute the reflection and transmission coefficients of the metafilm.

Such generalized boundary conditions have been first developed in [Kuester, Mohamed, Piket-May and Holloway (2003)], based on the dipole approximation of the individual meta-atoms of the metafilm. Apart from this important contribution, the authors of this work have also presented a simple procedure for the determination of the surface susceptibility matrix for arbitrary non-bianisotropic scatterers. This process, which can be regarded as the 2-D translation of the well-known Clausius-Mossotti formulas of the classical mixing theory [Sihvola (1999)], assumes only quasistatic electromagnetic interactions between meta-atoms. Two years later, analytical expressions for the reflection and transmission coefficients of such metafilms have been derived in [Holloway, Mohamed, Kuester and Dienstfrey (2005)], thus completing the first general-purpose surface susceptibility model. Furthermore, the extension of this model to bianisotropic scatterers has been presented in [Belokopytov, Zhuravlev and Terekhov (2011)], in which the cross-polarized reflection and transmission coefficients of a metafilm have also been evaluated. Similar results to the latter paper have been published in [Koledintseva, Huang, Drewniak, DuBroff and Archambeault (2012)], where the more general form of the metafilm's boundary conditions has also been introduced.

An alternative approach has been suggested in [Holloway, Dienstfrey, Kuester, O'Hara, Azad and Taylor (2009)], according to which the desired surface susceptibilities can be directly retrieved from the simulated values of the reflection and transmission coefficients of the metafilm. To this aim, the previously reported analytical expressions of the scattering coefficients [Holloway, Mohamed, Kuester and Dienstfrey (2005)] have been properly inverted. This extraction technique, which is − to some extent − similar to the well-known Nicolson-Ross-Weir retrieval algorithms for bulk metamaterials, has been proven very reliable and also applicable to realistic scatterer arrays, imprinted on a substrate material. Moreover, it has been successfully employed for the electromagnetic characterization of two parallel metafilms with shperical nanoparticles, located on the opposite sides of a dielectric substrate [Morits and Simovski (2010)]. However, the main shortcoming of this algorithm is that it has been rigorously developed only for structures with non-bianisotropic particles, thus restricting its general applicability.

Another analytical method has been proposed in our latest works [Dimitriadis, Sounas, Kantartzis, Caloz and Tsiboukis (2012); Dimitriadis, Kantartzis and Tsiboukis (2013)]. Contrary to the other models, this technique results in a set of non-local effective susceptibilities, namely parameters which depend on the incident wavevector. Despite the fact that these parameters do not represent meaningful physical entities, characteristic of the specific structure, they have been proven very efficient in the prediction of the reflection and transmission properties of metafilms. The key difference is the availability of a large number of off-diagonal matrix components, which can flexibly model the weak spatial dispersion phenomena, usually associated with such devices. Nevertheless, this approach has been previously presented only for specific metafilms illuminated by a TE-polarized plane wave.

In this paper, we review the most important aspects of the three general surface susceptibility models mentioned above, which are exclusively founded on the dipole approximation of the constituting meta-atoms. The structure of the paper is as follows: In Section 2, we provide a brief introduction to the dipole approximation technique and the properties of the corresponding particle polarizabilities. The differences between the two existing types of polarizabilities, i.e. the quasistatic and the dynamic ones, are carefully addressed, by providing, also, the basic principles that apply to each category. In Section 3, the three prescribed models are more elaborately present, highlighting possible implementation issues and other important traits. The third approach (the "proposed" technique) is adequately generalized compared to its structure-specific form in our previous publications. Furthermore, in Section 4, the three algorithms are implemented and extensively compared for various structures with lossless and lossy particles of increased practical interest. Their outcomes are also certified via numerical simulations, acquired by means of a

commercial computational suite. In the process, a set of new analytical formulas for the scattering coefficients of metafilms, comprising magneto-dielectric spheres and Ω-shaped bianisotropic particles, are derived and many novel physical insights on the phenomena under study are provided. Finally, in Section 5, we briefly summarize the main conclusions deduced during our investigation. Note that throughout the following analysis an $e^{j\omega t}$ time dependence is assumed and suppressed.

2 Polarizabilities of electrically-small scatterers

Prior to introducing the different surface susceptibility models for the electromagnetic characterization of a metafilm, we should, first, focus on the building blocks of such periodic structures, namely the meta-atoms. The properties of the individual particles are indeed very important, since they significantly affect the behavior of the overall device. The periodicity in metafilms is not as crucial a factor as in the traditional frequency selective surfaces (FSSs), because it only affects the strength of the inter-particle interactions on the lattice. In principle, periodicity is not even necessary for the operation of a metafilm, although it is usually preferable, in order to facilitate the analysis and fabrication procedures.

For the scatterers themselves, the most critical parameters are their shape and the electric/magnetic properties of the materials from which they are made. However, these parameters are not convenient for a unified description of such periodic arrays and hence, the latter are typically modeled via the classical multipole theory [Raab and De Lange (2005)]. According to this approach, charges and currents, induced on an isolated scatterer by externally-applied electromagnetic fields, can be expressed as the superposition of various polarization terms with increasing order of complexity (dipole, quadrupole, octopole etc.). The proportionality factors between these polarization moments and the externally applied electromagnetic fields are called polarizabilities and are tensors of increasing rank (second-rank for dipole polarizabilities, third-rank for quadrupole polarizabilities and so on).

In this paper, we examine only metafilm models which have been developed under the dipole approximation of the constitutive meta-atoms. The main parameters and notations of this approach are briefly introduced in the following subsections.

2.1 Dipole approximation

If a meta-atom is sufficiently smaller than the free-space wavelength of the impinging radiation (typically $D \leq \lambda/4$, where D is the largest dimension of the particle), its electromagnetic response to any external excitation can be modeled via the point-dipole approximation [Collin (1991)]. Specifically, each scatterer of the array may be substituted by an electric dipole moment, $\mathbf{p}$, and a magnetic dipole momen-

t, **m**, which are placed on its geometrical center. According to this approximation, these dipole moments can be related to the local field acting at the center of every scatterer[1] as in [Tretyakov (2003)]

$$\begin{bmatrix} \mathbf{p} \\ c_0^{-1}\mathbf{m} \end{bmatrix} = \begin{bmatrix} \bar{\bar{\alpha}}_{ee} & \bar{\bar{\alpha}}_{em} \\ \bar{\bar{\alpha}}_{me} & \bar{\bar{\alpha}}_{mm} \end{bmatrix} \cdot \begin{bmatrix} \varepsilon_0 \mathbf{E}^{\mathrm{loc}} \\ c_0^{-1}\mathbf{H}^{\mathrm{loc}} \end{bmatrix} \qquad \text{or} \qquad \boldsymbol{\mu} = [\alpha]\mathbf{f}^{\mathrm{loc}}, \tag{1}$$

where $c_0 = 1/\sqrt{\mu_0\varepsilon_0}$ the speed of light in vacuum, $\bar{\bar{\alpha}}_{ee}$, $\bar{\bar{\alpha}}_{em}$, $\bar{\bar{\alpha}}_{me}$, and $\bar{\bar{\alpha}}_{mm}$ are the electric-electric, electric-magnetic, magnetic-electric, and magnetic-magnetic second-rank dipole polarizability tensors of the particle, correspondingly, $[\alpha]$ is the total dipole[2] polarizability matrix, and

$$\boldsymbol{\mu} = \left[p_x, p_y, p_z, c_0^{-1}m_x, c_0^{-1}m_y, c_0^{-1}m_z\right]^T, \tag{2a}$$

$$\mathbf{f}^{\mathrm{loc}} = \left[\varepsilon_0 E_x^{\mathrm{loc}}, \varepsilon_0 E_y^{\mathrm{loc}}, \varepsilon_0 E_z^{\mathrm{loc}}, c_0^{-1}H_x^{\mathrm{loc}}, c_0^{-1}H_y^{\mathrm{loc}}, c_0^{-1}H_z^{\mathrm{loc}}\right]^T, \tag{2b}$$

are the normalized dipole moments and local fields six-vectors, respectively.

Note that, even in this first-order approximation, the complete description of a specific scatterer requires the knowledge of 36 complex polarizabilities in (1). However, for the vast majority of particles, most of these parameters are negligibly small. Furthermore, the reciprocity theorem enforces several limitations to the polarizability tensors, since the following symmetries and anti-symmetries must apply [Serdyukov, Semchenko, Tretyakov and Sihvola (2001)]

$$\bar{\bar{\alpha}}_{ee} = \bar{\bar{\alpha}}_{ee}^T, \qquad \bar{\bar{\alpha}}_{mm} = \bar{\bar{\alpha}}_{mm}^T, \qquad \bar{\bar{\alpha}}_{em} = -\bar{\bar{\alpha}}_{me}^T. \tag{3}$$

These formulas are known in the literature as the Onsager-Casimir principle and can be easily derived from the corresponding symmetries of the dyadic Green functions [Seršić, Tuambilangana, Kampfrath and Koenderink (2011)]. As a result, the total number of independent polarizability terms may be reduced from 36 to 21 complex parameters, in the more general case. For lossless particles as well as for specific geometries, like the planar metallic particles, further simplifications of the polarizability matrix are possible.

2.2 Quasistatic and dynamic polarizabilities

We should, now, distinguish between two different types of polarizabilities that we will encounter. The first category includes the polarizabilities which are developed

[1] This local field is the superposition of the external excitation and the sum of the scattered fields microscopically produced by every single scatterer of the array.

[2] Henceforth, the prefix "dipole" will be implied and omitted in front of the term "polarizability".

via the use of equivalent circuit models, like the *RLC* equivalent circuits of diverse split-ring resonators [Marqués, Martín and Sorolla (2008)]. Despite the fact that these models can predict the location of the first particle resonance with decent accuracy, they are limited by the assumption $c_0 = \infty$ (or, equally $k_0 = 0$) of lumped circuit models. This leads to inaccurate results when retardation effects significantly influence the performance of the structure, as is usually the case in various metamaterial devices. For this reason, these polarizabilities are not the most adequate choice for the study of the electrodynamic behavior of metafilms. In the rest of our work, we will refer to such polarizabilities as quasistatic, a term coined in [Seršić, Tuambilangana, Kampfrath and Koenderink (2011)].

Conversely, to study metafilms where the retardation effects should be properly taken into account, a set of dynamic polarizabilities is required. These parameters should − by definition − match some important criteria: (1) involve the speed of light (or, equivalently, the wavenumber, k_0) as a parameter, (2) satisfy the reciprocity theorem, in the form of the Onsager-Casimir principle, and (3) satisfy the energy conservation theorem. In the case of a lossless particle and to comply with (3), the polarizability tensors should be related to each other through the so-called Sipe-Kranendonk conditions [Belov, Maslovski, Simovski and Tretyakov (2003)]

$$\mathrm{Im}\left\{ \left(\bar{\bar{\alpha}}_{ee} - \bar{\bar{\alpha}}_{em} \bar{\bar{\alpha}}_{mm}^{-1} \bar{\bar{\alpha}}_{me} \right)^{-1} \right\} = \frac{k_0^3}{6\pi} \bar{\bar{I}}, \tag{4a}$$

$$\mathrm{Im}\left\{ \left(\bar{\bar{\alpha}}_{mm} - \bar{\bar{\alpha}}_{me} \bar{\bar{\alpha}}_{ee}^{-1} \bar{\bar{\alpha}}_{em} \right)^{-1} \right\} = \frac{k_0^3}{6\pi} \bar{\bar{I}}, \tag{4b}$$

$$\mathrm{Re}\left\{ \left(\bar{\bar{\alpha}}_{ee} - \bar{\bar{\alpha}}_{em} \bar{\bar{\alpha}}_{mm}^{-1} \bar{\bar{\alpha}}_{me} \right)^{-1} \bar{\bar{\alpha}}_{em} \bar{\bar{\alpha}}_{mm}^{-1} \right\} = \bar{\bar{0}}. \tag{4c}$$

In the special case of non-bianisotropic scatterers, when $\bar{\bar{\alpha}}_{em} = \bar{\bar{\alpha}}_{me} = \bar{\bar{0}}$, these expressions are simplified to

$$\mathrm{Im}\left\{ \bar{\bar{\alpha}}_{ee}^{-1} \right\} = \frac{k_0^3}{6\pi} \bar{\bar{I}} \qquad \text{and} \qquad \mathrm{Im}\left\{ \bar{\bar{\alpha}}_{mm}^{-1} \right\} = \frac{k_0^3}{6\pi} \bar{\bar{I}}. \tag{5}$$

It should be stressed that the quasistatic polarizabilities of a particle do not satisfy these criteria, since, in this case, the polarizability tensors are either purely real ($\bar{\bar{\alpha}}_{ee}$, $\bar{\bar{\alpha}}_{mm}$) or purely imaginary ($\bar{\bar{\alpha}}_{em}$, $\bar{\bar{\alpha}}_{me}$) [Marqués, Martín and Sorolla (2008)]. The Onsager-Casimir principle applies, of course, to both types of polarizabilities, as it arises from the reciprocity principle.

Finally, we should mention two important techniques that will be systematically employed in the rest of the paper. The first one, proposed in [Seršić, Tuambilangana, Kampfrath and Koenderink (2011)], concerns the transformation of the quasistatic polarizabilities of a lossless scatterer into the corresponding dynamic ones.

This can be done by properly adding the radiation damping term to the quasistatic polarizability matrix, which can be mathematically described as

$$[\alpha]_{\text{dyn}}^{-1} = [\alpha]_{\text{stat}}^{-1} + j\frac{k_0^3}{6\pi}\bar{\bar{I}}. \tag{6}$$

Such a procedure is applicable in any case, provided that the polarizability matrix can be inverted. Since, for many realistic scatterers, most of the 36 elements of $[\alpha]$ are zero, the latter frequently reduces to a square matrix of lower order (for example 4×4 or 3×3). In these cases, the reduced matrix needs to be invertible, as the full 6×6 one is obviously singular and cannot be inverted.

The second technique, introduced in [Yatsenko, Maslovski, Tretyakov, Prosvirnin and Zouhdi (2003)], refers to the inverse procedure, namely the determination of the quasistatic polarizabilites of a lossless particle, given its dynamic polarizability matrix. Nevertheless, contrary to the previous case, this technique can only be applied in some special cases, as it requires the solution of a system of equations, which is not always invertible.

3 Effective surface susceptibility models

Let us, now, consider the actual problem of an infinite periodic metafilm in free space, which is assumed to coincide with the $z=0$ plane, as in Fig. 1. The most efficient way of modeling such structures is in terms of effective surface parameters, that relate the field components at their two sides through a generalized boundary condition. To reach such conditions, we start from the classical discontinuity boundary conditions for a thin slab of homogeneous material, located between the $z=-d/2$ and $z=d/2$ planes. If this slab is excited from an arbitrary electromagnetic field, the field components on the $z=d/2$ face (similarly for the $z=-d/2$ face) will satisfy the relations [Collin (1991)]

$$\hat{\mathbf{z}}\times\left(\mathbf{H}|_{z=d/2^+}-\mathbf{H}|_{z=d/2^-}\right)=\mathbf{J}_s, \tag{7a}$$

$$\hat{\mathbf{z}}\times\left(\mathbf{E}|_{z=d/2^+}-\mathbf{E}|_{z=d/2^-}\right)=-\mathbf{K}_s, \tag{7b}$$

with $\mathbf{J}_s$ and $\mathbf{K}_s$ the electric and magnetic surface currents, respectively, induced on the boundary surface. For a metafilm under the dipole approximation, followed herein, these surface currents can be related to the (electric) surface polarization, $\mathbf{P}_s$, and magnetization, $\mathbf{M}_s$, vectors induced on its surface. Thus, letting also $d\to 0$, (7) can be written as [Idemen (1988)]

$$\hat{\mathbf{z}}\times(\mathbf{H}|_{z=0^+}-\mathbf{H}|_{z=0^-})=j\omega\mathbf{P}_{st}-\hat{\mathbf{z}}\times\nabla_t M_{sz}, \tag{8a}$$

$$\hat{\mathbf{z}}\times(\mathbf{E}|_{z=0^+}-\mathbf{E}|_{z=0^-})=-j\omega\mu_0\mathbf{M}_{st}-\hat{\mathbf{z}}\times\nabla_t(P_{sz}/\varepsilon_0), \tag{8b}$$

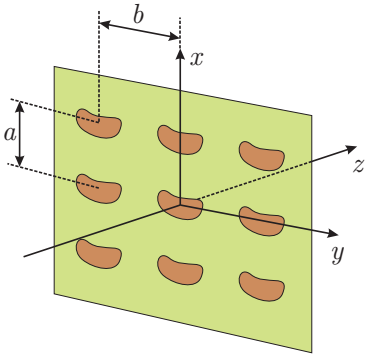

Figure 1: Geometry of an arbitrary periodic metafilm located on the $z = 0$ plane.

where the index t refers to the tangential components of the surface polarizations/magnetizations or differential operators.

Next, if we define the effective surface susceptibilities as

$$\mathbf{P}_s = \varepsilon_0 \bar{\bar{\chi}}_{ee} \cdot \overline{\mathbf{E}}, \qquad \bar{\bar{\chi}}_{ee} = \mathrm{diag}\left\{\chi_{ee}^{xx}, \chi_{ee}^{yy}, \chi_{ee}^{zz}\right\}, \tag{9a}$$

$$\mathbf{M}_s = \bar{\bar{\chi}}_{mm} \cdot \overline{\mathbf{H}}, \qquad \bar{\bar{\chi}}_{mm} = \mathrm{diag}\left\{\chi_{mm}^{xx}, \chi_{mm}^{yy}, \chi_{mm}^{zz}\right\}, \tag{9b}$$

with $\overline{\mathbf{E}}$ and $\overline{\mathbf{H}}$ denoting the average electric and magnetic fields at the two faces of the metafilm, (8) become [Kuester, Mohamed, Piket-May and Holloway (2003)]

$$\hat{\mathbf{z}} \times \mathbf{H}|_{z=0^-}^{0^+} = j\omega\varepsilon_0 \left(\bar{\bar{\chi}}_{ee}\right)_t \cdot \overline{\mathbf{E}}_t - \hat{\mathbf{z}} \times \nabla_t \left(\chi_{mm}^{zz} \overline{H}_z\right), \tag{10a}$$

$$\hat{\mathbf{z}} \times \mathbf{E}|_{z=0^-}^{0^+} = -j\omega\mu_0 \left(\bar{\bar{\chi}}_{mm}\right)_t \cdot \overline{\mathbf{H}}_t - \hat{\mathbf{z}} \times \nabla_t (\chi_{ee}^{zz} \overline{E}_z). \tag{10b}$$

However, note that (9) are valid only for metafilms comprising biaxially anisotropic meta-atoms. For the more general case of bianisotropic metafilms, 4 surface susceptibility tensors are required, which can be defined from [Dimitriadis, Sounas, Kantartzis, Caloz and Tsiboukis (2012)]

$$\begin{bmatrix} \mathbf{P}_s \\ c_0^{-1}\mathbf{M}_s \end{bmatrix} = \begin{bmatrix} \bar{\bar{\chi}}_{ee} & \bar{\bar{\chi}}_{em} \\ \bar{\bar{\chi}}_{me} & \bar{\bar{\chi}}_{mm} \end{bmatrix} \cdot \begin{bmatrix} \varepsilon_0 \overline{\mathbf{E}} \\ c_0^{-1} \overline{\mathbf{H}} \end{bmatrix} \qquad \text{or} \qquad \boldsymbol{\mu}_s = [\chi] \bar{\mathbf{f}} \tag{11}$$

where

$$\boldsymbol{\mu}_s = [P_{sx}, P_{sy}, P_{sz}, c_0^{-1}M_{sx}, c_0^{-1}M_{sy}, c_0^{-1}M_{sz}]^T, \tag{12a}$$

$$\bar{\mathbf{f}} = \left[\varepsilon_0 \overline{E}_x, \varepsilon_0 \overline{E}_y, \varepsilon_0 \overline{E}_z, c_0^{-1}\overline{H}_x, c_0^{-1}\overline{H}_y, c_0^{-1}\overline{H}_z\right]^T, \tag{12b}$$

are the normalized surface polarization/magnetization and average field six-vectors, respectively. Plugging the prior expressions into (8), we finally obtain [Koledintseva, Huang, Drewniak, DuBroff and Archambeault (2012)]

$$\hat{\mathbf{z}}\times\mathbf{H}|_{z=0^-}^{0^+} = j\omega\left[\left(\boldsymbol{\chi}_e^x\cdot\bar{\mathbf{f}}\right)\hat{\mathbf{x}}+\left(\boldsymbol{\chi}_e^y\cdot\bar{\mathbf{f}}\right)\hat{\mathbf{y}}\right]-\hat{\mathbf{z}}\times c_0\nabla_t\left(\boldsymbol{\chi}_m^z\cdot\bar{\mathbf{f}}\right), \tag{13a}$$

$$\hat{\mathbf{z}}\times\mathbf{E}|_{z=0^-}^{0^+} = -j\omega\eta_0\left[\left(\boldsymbol{\chi}_m^x\cdot\bar{\mathbf{f}}\right)\hat{\mathbf{x}}+\left(\boldsymbol{\chi}_m^y\cdot\bar{\mathbf{f}}\right)\hat{\mathbf{y}}\right]-\hat{\mathbf{z}}\times\varepsilon_0^{-1}\nabla_t\left(\boldsymbol{\chi}_e^z\cdot\bar{\mathbf{f}}\right), \tag{13b}$$

with $\boldsymbol{\chi}_i^j = \left[\chi_{ie}^{jx}\ \chi_{ie}^{jy}\ \chi_{ie}^{jz}\ \chi_{im}^{jx}\ \chi_{im}^{jy}\ \chi_{im}^{jz}\right]^T$, for $i=\{e,m\}$ and $j=\{x,y,z\}$, the rows of $[\chi]$ in (11) and $\eta_0=\sqrt{\mu_0/\varepsilon_0}$. These are the more general boundary conditions within the dipole approximation technique and suffice for the solution of any metafilm scattering problem, provided that $[\chi]$ can be determined. Subsequently, we present the most common methods for the derivation of $[\chi]$.

3.1 Quasistatic interaction model

Consider a metafilm, formed by the periodic repetition of biaxially anisotropic meta-atoms which are described by the polarizability matrix

$$[\alpha] = \mathrm{diag}\{\alpha_{ee}^{xx},\alpha_{ee}^{yy},\alpha_{ee}^{zz},\alpha_{mm}^{xx},\alpha_{mm}^{yy},\alpha_{mm}^{zz}\}. \tag{14}$$

Following an analytical procedure for the calculation of the local field, acting on a single scatterer of the lattice, the authors of [Kuester, Mohamed, Piket-May and Holloway (2003)] have proven that the elements of the surface susceptibility matrix $[\chi]$ that describes the metafilm may be computed via

$$\chi_{ii}^{xx} = \frac{N\alpha_{ii}^{xx}}{1-\frac{N\alpha_{ii}^{xx}}{4R}}, \qquad \chi_{ii}^{yy} = \frac{N\alpha_{ii}^{yy}}{1-\frac{N\alpha_{ii}^{yy}}{4R}}, \qquad \chi_{ii}^{zz} = \frac{N\alpha_{ii}^{zz}}{1+\frac{N\alpha_{ii}^{zz}}{2R}}, \tag{15}$$

where $i=(e,m)$, $N=(ab)^{-1}$ is the number of scatterers per unit surface, and R the radius of a circular disk, whose center is located on the scatterer where the local field is calculated. This radius depends on the periodicities of the structure and, for the special case of a square lattice ($a=b$), it takes the value $R=0.6956a$ [Collin (1991)]. It is worth mentioning that, for the derivation of (15), the quasistatic approximation $k_0R\ll 1$ has been made, thus justifying the name usually attributed to this technique. Moreover, the analogy of (15) to the well-known Clausius-Mossotti mixing rule [Sihvola (1999)] is evident, as the only difference lies on the values of the depolarization tensor of the circular disk ($\bar{\bar{L}}=\mathrm{diag}\{1/4R,1/4R,-1/2R\}$), compared to the depolarization tensor of the sphere.

The extension of the above technique to the more general case of bianisotropic scatterers has been performed in [Belokopytov, Zhuravlev and Terekhov (2011)].

Selecting a similar methodology, its authors reached the matrix formula of

$$[\chi] = [\beta]^{-1} N[\alpha], \tag{16}$$

with the elements of $[\beta]$ matrix defined as

$$\beta_{ee}^{ij} = \delta_{ij} + N\alpha_{ee}^{ik} \cdot L_{kj}, \tag{17a}$$

$$\beta_{em}^{ij} = N\alpha_{em}^{ik} \cdot L_{kj}, \tag{17b}$$

$$\beta_{me}^{ij} = N\alpha_{me}^{ik} \cdot L_{kj}, \tag{17c}$$

$$\beta_{mm}^{ij} = \delta_{ij} + N\alpha_{mm}^{ik} \cdot L_{kj}, \tag{17d}$$

for $(i, j) = (x, y, z)$, where δ_{ij} is the Kronecker delta and the notation $\alpha_{ee}^{ik} \cdot L_{kj}$ implies the dot product of the i-th row of $\bar{\bar{\alpha}}_{ee}$ with the j-th column of the depolarization tensor of the circular disk, $\bar{\bar{L}}$ (likewise for the other polarizability tensors).

Observe that, for the computation of surface susceptibility matrix $[\chi]$ through this quasistatic approach, it is necessary to know the quasistatic polarizability matrix $[\alpha]'$ of the constituting meta-atom and the lattice parameters of the metafilm. It should be stressed that, in the case of lossless metafilms, if the dynamic polarizability matrix $[\alpha]$ of the scatterer is utilized instead of its quasistatic counterpart, the parameters derived from (15) and (16) do not satisfy the energy conservation law, and lead to an incorrect modeling of the structure. When this pitfall is avoided, the resulting parameters of the model should comply with the locality conditions and may be treated as characteristic parameters of the metafilm, since they are independent on its excitation [Simovski and Tretyakov (2007)]. In what follows, this technique will be referred to as the "K-B method", from the initial letters of the first authors in the aforementioned publications.

3.2 S-parameter retrieval algorithm

Another approach for the calculation of the surface susceptibility matrix $[\chi]$ of a metafilm, that contains biaxially anisotropic scatterers, has been proposed in [Holloway, Dienstfrey, Kuester, O'Hara, Azad and Taylor (2009)]. Essentially, it is based on the inversion of the analytical expressions for the reflection and transmission coefficients. The latter can be obtained by inserting the field expressions for the incident, reflected, and transmitted waves into the boundary conditions (10), as explained in [Holloway, Mohamed, Kuester and Dienstfrey (2005)]. Then, by solving the resulting systems of equations for the perpendicular (Fig. 2(a)) and the parallel (Fig. 2(b)) polarization, we obtain

$$R_{\perp}(\theta) = \frac{-j\frac{k_0}{2\cos\theta}\left(\chi_{ee}^{xx} - \chi_{mm}^{yy}\cos^2\theta + \chi_{mm}^{zz}\sin^2\theta\right)}{1 - \left(\frac{k_0}{2}\right)^2 \chi_{mm}^{yy}\left(\chi_{ee}^{xx} + \chi_{mm}^{zz}\sin^2\theta\right) + j\frac{k_0}{2\cos\theta}\left(\chi_{ee}^{xx} + \chi_{mm}^{yy}\cos^2\theta + \chi_{mm}^{zz}\sin^2\theta\right)}, \tag{18a}$$

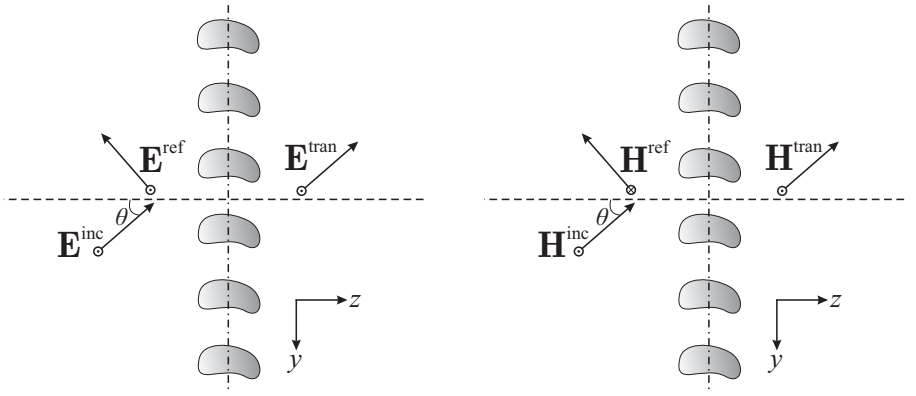

(a) (b)

Figure 2: Incident, reflected, and transmitted waves for an arbitrary periodic metafilm. (a) Perpendicular and (b) parallel polarization.

$$T_{\perp}(\theta)=\frac{1+\left(\frac{k_0}{2}\right)^2\chi_{mm}^{yy}\left(\chi_{ee}^{xx}+\chi_{mm}^{zz}\sin^2\theta\right)}{1-\left(\frac{k_0}{2}\right)^2\chi_{mm}^{yy}\left(\chi_{ee}^{xx}+\chi_{mm}^{zz}\sin^2\theta\right)+j\frac{k_0}{2\cos\theta}\left(\chi_{ee}^{xx}+\chi_{mm}^{yy}\cos^2\theta+\chi_{mm}^{zz}\sin^2\theta\right)}, \quad (18b)$$

$$R_{\parallel}(\theta)=\frac{-j\frac{k_0}{2\cos\theta}\left(\chi_{mm}^{xx}-\chi_{ee}^{yy}\cos^2\theta+\chi_{ee}^{zz}\sin^2\theta\right)}{1-\left(\frac{k_0}{2}\right)^2\chi_{ee}^{yy}\left(\chi_{mm}^{xx}+\chi_{ee}^{zz}\sin^2\theta\right)+j\frac{k_0}{2\cos\theta}\left(\chi_{mm}^{xx}+\chi_{ee}^{yy}\cos^2\theta+\chi_{ee}^{zz}\sin^2\theta\right)}, \quad (19a)$$

$$T_{\parallel}(\theta)=\frac{1+\left(\frac{k_0}{2}\right)^2\chi_{ee}^{yy}\left(\chi_{mm}^{xx}+\chi_{ee}^{zz}\sin^2\theta\right)}{1-\left(\frac{k_0}{2}\right)^2\chi_{ee}^{yy}\left(\chi_{mm}^{xx}+\chi_{ee}^{zz}\sin^2\theta\right)+j\frac{k_0}{2\cos\theta}\left(\chi_{mm}^{xx}+\chi_{ee}^{yy}\cos^2\theta+\chi_{ee}^{zz}\sin^2\theta\right)}, \quad (19b)$$

where θ is the incidence angle on the yz-plane. If these coefficients are determined for a normal incidence ($\theta=0^\circ$) and for another arbitrary angle of incidence θ, (18) and (19) can be inverted, and the surface susceptibilities read

$$\chi_{ee}^{xx}=\frac{2j}{k_0}\frac{R_{\perp}(0)+T_{\perp}(0)-1}{R_{\perp}(0)+T_{\perp}(0)+1}, \qquad \chi_{mm}^{xx}=\frac{2j}{k_0}\frac{R_{\parallel}(0)-T_{\parallel}(0)+1}{R_{\parallel}(0)-T_{\parallel}(0)-1}, \quad (20a)$$

$$\chi_{ee}^{yy}=\frac{2j}{k_0}\frac{R_{\parallel}(0)+T_{\parallel}(0)-1}{R_{\parallel}(0)+T_{\parallel}(0)+1}, \qquad \chi_{mm}^{yy}=\frac{2j}{k_0}\frac{R_{\perp}(0)-T_{\perp}(0)+1}{R_{\perp}(0)-T_{\perp}(0)-1}, \quad (20b)$$

$$\chi_{ee}^{zz}=-\frac{\chi_{mm}^{xx}}{\sin^2\theta}-\frac{2j\cos\theta}{k_0\sin^2\theta}\frac{R_{\parallel}(\theta)-T_{\parallel}(\theta)+1}{R_{\parallel}(\theta)-T_{\parallel}(\theta)-1}, \quad (20c)$$

$$\chi_{mm}^{zz}=-\frac{\chi_{ee}^{xx}}{\sin^2\theta}+\frac{2j\cos\theta}{k_0\sin^2\theta}\frac{R_{\perp}(\theta)+T_{\perp}(\theta)-1}{R_{\perp}(\theta)+T_{\perp}(\theta)+1}. \quad (20d)$$

It is mentioned that, for the computation of $[\chi]$ tangential components, only the scattering coefficients of normally incident waves are required, while for the normal components it is necessary to use the coefficients of an obliquely incident wave ($\theta \neq 0$), as well. These parameters are, also, local and are − in theory − independent on the selection of θ. However, in practice, the values of normal components χ_{ee}^{zz} and χ_{mm}^{zz} are different for various θ, and they are additionally proven very sensitive to the numerical noise of the scattering coefficients, as later discussed.

Finally, the authors of [Morits and Simovski (2010)] have successfully applied this method in the electromagnetic characterization of a bi-layered metafilm, i.e. a structure comprising two closely-spaced arrays of magneto-dielectric spheres. Nonetheless, to the best of our knowledge, this approach has not yet been applied to metafilms with bianisotropic scatterers, since the corresponding analytical expressions for the reflection and transmission coefficients are too complicated to be inverted. In what follows, we will use the abbreviation "H-M method", when referring to the technique described in this subsection.

3.3 Dynamic non-local approach

Recently, we have developed an efficient algorithm for the electromagnetic characterization of metafilms consisting of biaxially anisotropic [Dimitriadis, Sounas, Kantartzis, Caloz and Tsiboukis (2012)] and planar bianisotropic [Dimitriadis, Kantartzis and Tsiboukis (2013)] scatterers. This method is based on the combination of an analytical microscopic modeling approach, which accurately accounts for the dynamic dipolar interactions between the meta-atoms in the lattice, with a rigorous macroscopic averaging procedure, in order to obtain the desired surface susceptibility matrix. However, the analysis in these works has been performed only for TE-polarized incident waves and for some special cases of constituting particles, thus limiting the general applicability of the overall formulation. Here, we settle this issue by presenting generalized expressions, valid for any periodic metafilm and plane wave excitation of arbitrary polarization.

To this objective, the surface susceptibility matrix is evaluated from

$$[\chi] = \left\{ (ab)[\alpha]^{-1} - (ab)[C] + [D] \right\}^{-1}, \tag{21}$$

where $[\alpha]$ is the dynamic polarizability matrix, $[D]$ is the jump condition matrix

$$[D] = \begin{bmatrix} \frac{-jk_0^2}{2k_z} & 0 & 0 & 0 & 0 & \frac{jk_0k_y}{2k_z} \\ 0 & \frac{-jk_z}{2} & 0 & 0 & 0 & 0 \\ 0 & 0 & \frac{-jk_y^2}{2k_z} & \frac{-jk_0k_y}{2k_z} & 0 & 0 \\ 0 & 0 & \frac{-jk_0k_y}{2k_z} & \frac{-jk_0^2}{2k_z} & 0 & 0 \\ 0 & 0 & 0 & 0 & \frac{-jk_z}{2} & 0 \\ \frac{jk_0k_y}{2k_z} & 0 & 0 & 0 & 0 & \frac{-jk_y^2}{2k_z} \end{bmatrix}, \tag{22}$$

and $[C]$ is the intraplanar interaction coefficient matrix, defined as

$$[C] = \begin{bmatrix} \bar{\bar{C}}_{ee} & \bar{\bar{C}}_{em} \\ \bar{\bar{C}}_{me} & \bar{\bar{C}}_{mm} \end{bmatrix} = \sum_{(m,n)\neq(0,0)} \begin{bmatrix} \bar{\bar{G}}^{(1)}(\mathbf{R}_{mn}) & \bar{\bar{G}}^{(2)}(\mathbf{R}_{mn}) \\ -\bar{\bar{G}}^{(2)}(\mathbf{R}_{mn}) & \bar{\bar{G}}^{(1)}(\mathbf{R}_{mn}) \end{bmatrix} e^{-jk_ynb}. \tag{23}$$

In this formula, $\bar{\bar{G}}^{(1)}(\mathbf{R}_{mn})$ and $\bar{\bar{G}}^{(2)}(\mathbf{R}_{mn})$ represent the dyadic Green functions

$$\bar{\bar{G}}^{(1)}(\mathbf{R}_{mn}) = \left(k_0^2\bar{\bar{I}} + \nabla\nabla\right) g_0(\mathbf{R}_{mn}), \tag{24a}$$

$$\bar{\bar{G}}^{(2)}(\mathbf{R}_{mn}) = -jk_0\nabla g_0(\mathbf{R}_{mn}) \times \bar{\bar{I}}, \tag{24b}$$

and $g_0(\mathbf{R}_{mn})$ corresponds to the scalar Green function of free space

$$g_0(\mathbf{R}_{mn}) = \frac{e^{-jk_0|\mathbf{R}_{mn}|}}{4\pi|\mathbf{R}_{mn}|}, \tag{25}$$

where $\mathbf{R}_{mn}$ is the vector pointing from (m,n) to $(0,0)$. From the above expressions, it follows that only half of the elements of $[C]$ are non-zero, namely

$$[C] = \begin{bmatrix} C_{ee}^{xx} & C_{ee}^{xy} & 0 & 0 & 0 & C_{em}^{xz} \\ C_{ee}^{yx} & C_{ee}^{yy} & 0 & 0 & 0 & C_{em}^{yz} \\ 0 & 0 & C_{ee}^{zz} & C_{em}^{zx} & C_{em}^{zy} & 0 \\ 0 & 0 & C_{me}^{xz} & C_{mm}^{xx} & C_{mm}^{yx} & 0 \\ 0 & 0 & C_{me}^{yz} & C_{mm}^{xy} & C_{mm}^{yy} & 0 \\ C_{me}^{zx} & C_{me}^{zy} & 0 & 0 & 0 & C_{mm}^{zz} \end{bmatrix}. \tag{26}$$

Furthermore, due to the reciprocity principle, dyadic Green functions $\bar{\bar{G}}^{(1)}(\mathbf{R}_{mn})$ and $\bar{\bar{G}}^{(2)}(\mathbf{R}_{mn})$ must fulfill the following symmetry conditions

$$\left[\bar{\bar{G}}^{(1)}(\mathbf{R}_{mn})\right]^T = \bar{\bar{G}}^{(1)}(\mathbf{R}_{mn}), \qquad \left[\bar{\bar{G}}^{(2)}(\mathbf{R}_{mn})\right]^T = -\bar{\bar{G}}^{(2)}(\mathbf{R}_{mn}), \tag{27}$$

which lead to the corresponding relations between the elements of $[C]$ in (26)

$$\bar{\bar{C}}_{ee}^{T} = \bar{\bar{C}}_{ee} \equiv \bar{\bar{C}}_{mm}^{T} = \bar{\bar{C}}_{mm}, \quad \bar{\bar{C}}_{em}^{T} = -\bar{\bar{C}}_{em} \equiv \bar{\bar{C}}_{me}, \quad \bar{\bar{C}}_{me}^{T} = -\bar{\bar{C}}_{me} \equiv \bar{\bar{C}}_{em}. \tag{28}$$

Finally, by taking also into account the rotational symmetries of the dipole interaction problem, is has been shown in [Scher (2008)] that only the computation of 4 independent parameters is required (C_{ee}^{xx}, C_{ee}^{zz}, C_{ee}^{yx}, and C_{me}^{zx}), in order to fully determine the elements of $[C]$ in (26). Expressions for the calculation of these dynamic interaction coefficients, by means of rapidly-convergent series, can be found in various publications in the literature [Belov and Simovski (2005); Scher (2008); Dimitriadis, Sounas, Kantartzis, Caloz and Tsiboukis (2012)]. It should be stressed that both $[C]$ and $[D]$ matrices are always symmetric, irrespective of the specific microscopic geometry of the structure and the form of its excitation.

Hence, the matrix formula (21) indicates that $[\chi]$ can be obtained as the superposition of three terms with distinct physical meaning: $[\alpha]$, representing the microscopic properties of every individual scatterer, $[C]$, accounting for the dynamic intraplanar interactions between the meta-atoms, and $[D]$, expressing the field discontinuities across the metafilm in relation to the surface polarization and magnetization six-vector. Note that both $[C]$ and $[D]$ depend on the wavevector of the incident radiation. Therefore, contrary to the previous methods, the parameters of this model are non-local and cannot be treated as meaningful physical parameters of the structure. Nevertheless, they are more flexible and very instructive for the correct prediction of the reflection and transmission properties of various metafilms.

For the very important practical case of lossless metafilms, it can be proven that $[\chi]$ is an Hermitian matrix[3] and (21) can be simplified into

$$[\chi] = \left\{ ab \left([\alpha]^{-1} - \mathrm{Re}\{[C]\} - j\frac{k_0^3}{6\pi}[I] \right) \right\}^{-1}, \tag{29}$$

where $\mathrm{Re}\{\cdot\}$ defines the real part of a quantity and $[I]$ is the unitary matrix. If, additionally, the scatterers of the metafilm are non-bianisotropic ($\bar{\bar{\alpha}}_{em} = \bar{\bar{\alpha}}_{me} = \bar{\bar{0}}$), $[\chi]$ becomes also symmetric. This feature, together with the Hermitian property, leads to a purely real matrix $[\chi]$, that can be computed from

$$[\chi] = \left(ab\,\mathrm{Re}\left\{ [\alpha]^{-1} - [C] \right\} \right)^{-1}, \tag{30}$$

as follows from the Sipe-Kranendonk conditions of (5).

[3] This property, proven in the appendix of [Dimitriadis, Sounas, Kantartzis, Caloz and Tsiboukis (2012)], is valid for any surface susceptibility model.

Lastly, it is interesting to stress that, for metafilms formed by planar scatterers, the jump condition matrix reduces to the 3×3 form

$$[D] = \begin{bmatrix} -\frac{j(k_y^2+k_z^2)}{2k_z} & 0 & \frac{jk_0k_y}{2k_z} \\ 0 & \frac{-jk_z}{2} & 0 \\ \frac{jk_0k_y}{2k_z} & 0 & -\frac{jk_y^2}{2k_z} \end{bmatrix}, \tag{31}$$

and, similarly, the general expression for $[\chi]$ is written

$$[\chi] = \begin{bmatrix} \chi_{ee}^{xx} & \chi_{ee}^{xy} & \chi_{em}^{xz} \\ \chi_{ee}^{yx} & \chi_{ee}^{yy} & \chi_{em}^{yz} \\ \chi_{me}^{zx} & \chi_{me}^{zy} & \chi_{mm}^{zz} \end{bmatrix}. \tag{32}$$

In the next section, we will verify the validity of this generalized approach (henceforth called "proposed" method), in comparison to the aforementioned techniques.

4 Numerical results

In this section, we will extensively compare the aforementioned techniques for various cases of infinite lossless and lossy metafilms. Their outcomes will also be compared with the numerical results obtained from the commercial simulation package [CST MWS™ (2012)], which are considered as the reference solutions. In all simulations, a single unit-cell of the metafilm under study has been analyzed, by placing periodic boundary conditions (PBCs) at the $x = \pm a/2$ and $y = \pm b/2$ planes (see Fig. 1). This approach, which is fully equivalent to the study of an infinite periodic metafilm, stems from the Floquet-Bloch theory [Tretyakov (2003)] and is generally considered as an efficient approximation for the analysis of finite periodic structures as well, provided that the latter have minimum dimensions of about 2λ along the axes of the periodicity [Bhattacharyya (2014)].

Furthermore, the appropriate excitation ports have been placed at the $z = \pm\ell = \pm 3a$ planes, also considered as the reference planes for the phase of the reflection and transmission coefficients. Note, also, that our computational domain is terminated by applying perfectly-matched layers (PMLs), just after the excitation ports. The distance $\ell = 3a$ has been selected, in order to make sure that any evanescent mode, possibly radiated by the structure, is drastically attenuated before reaching the excitation ports and that the PMLs are properly functioning. Finally, for the implementation of the H-M method, a $\theta = 45^\circ$ angle has been chosen, in all cases, for the derivation of the parameters in (20c) and (20d).

4.1 Magneto-dielectric spheres

4.1.1 Lossless case

In first place, we investigate a metafilm comprising spherical magneto-dielectric meta-atoms. These particular scatterers have lately received an increasing scientific interest, since they can be successfully employed for the implementation of isotropic DNG materials [Holloway, Kuester, Baker-Jarvis and Kabos (2003); Shore and Yaghjian (2007)]. Moreover, they usually exhibit lower losses within the resonance band, compared to most of the − commonly used − metallic scatterers, and may be fabricated by utilizing ferrimagnetic materials with externally controllable properties, like the yttrium-iron garnet [Holloway, Kabos, Mohamed, Kuester, Gordon, Janezic and Baker-Jarvis (2010)]. Moreover, due to their canonical geometrical shape and the existence of analytical expressions for the calculation of their electric and magnetic polarizabilities, they constitute a convenient choice for testing the validity of various effective-medium theories [Alù (2011)].

So, let us presume a doubly-periodic repetition of the unit cell of Fig. 3(a) along the x and y directions. Initially, we consider a rather sparse distribution of lossless scatterers, consisting of a material with $\varepsilon_r = 13.8$ and $\mu_r = 11.0$, while the filling ratio of the unit cell is $\gamma = r/a = 0.15$, for r the radius of the spheres. The quasistatic polarizabilities of this particular meta-atom in free-space can be evaluated by the analytical formulas [Holloway, Mohamed, Kuester and Dienstfrey (2005)]

$$\alpha'_{ee} = 3V \frac{F(\varphi)\varepsilon_p - \varepsilon_0}{\varepsilon_p + 2\varepsilon_0}, \tag{33a}$$

$$\alpha'_{mm} = 3V \frac{F(\varphi)\mu_p - \mu_0}{\mu_p + 2\mu_0}, \tag{33b}$$

$$F(\varphi) = \frac{2(\sin\varphi - \varphi\cos\varphi)}{(\varphi^2 - 1)\sin\varphi + \varphi\cos\varphi}, \tag{33c}$$

where $V = 4\pi r^3/3$ is the volume of the sphere, ω is the angular frequency, $\varepsilon_p = \varepsilon_r\varepsilon_0$, $\mu_p = \mu_r\mu_0$, and $\varphi = \omega r\sqrt{\varepsilon_p\mu_p}$. These polarizabilities are depicted in Fig. 3(b) and can be directly used for the implementation of the K-B method, as explained in Section 3.1, whereas the respective dynamic polarizabilities may be obtained by "adding" the radiation damping term via the procedure of [Seršić, Tuambilangana, Kampfrath and Koenderink (2011)]. The latter, provided in Fig. 3(c), can be utilized for launching the proposed algorithm of Section 3.3. By comparing Figs 3(b) and 3(c), one may realize the effect of including the radiation losses in the expressions of the dynamic polarizabilities: the corresponding resonances become wider and less sharp in magnitude, compared to the quasistatic polarizabilities.

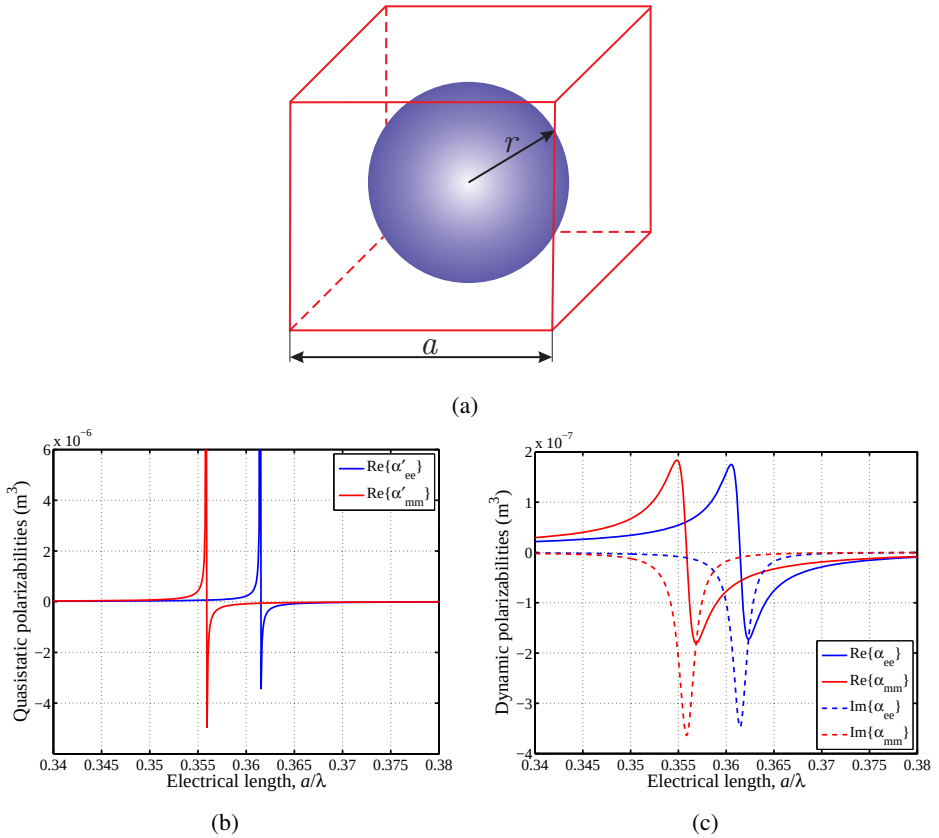

Figure 3: (a) Unit-cell of the metafilm under study with $a = 6\,\text{mm}$ and $r = 0.9\,\text{mm}$, (b) quasistatic, and (c) dynamic polarizabilities of a magneto-dielectric sphere made up of a material with $\varepsilon_r = 13.8$ and $\mu_r = 11.0$.

Next, we compare the computed surface susceptibilities of the three models under study. For those of the K-B (Figs 4(a) and 4(b)) and H-M (Figs 4(c) and 4(d)) methods , we observe that $\chi_{ee}^{xx} = \chi_{ee}^{yy}$ and $\chi_{mm}^{xx} = \chi_{mm}^{yy}$, as expected from the four-fold rotational symmetry of the unit-cell. Note that, despite the fact that both methods yield local effective parameters, which can be regarded as characteristic parameters of this specific metafilm, their parameters are not identical. Specifically, for the K-B method, the tangential components can be satisfactorily approximated via $\chi_{ii}^{jj} \approx \alpha_{ii}'/(ab)$, where $i = (e,m)$ and $j = (x,y)$. Thus, these parameters can be understood as a simple surface average of the corresponding polarizability terms, so justifying the classification of this approach as a quasistatic one. On the other hand, the H-M technique leads to a slightly shifted set of characteristic parameters. Moreover, χ_{ee}^{zz} and χ_{mm}^{zz} exhibit resonances in a second frequency region, name-

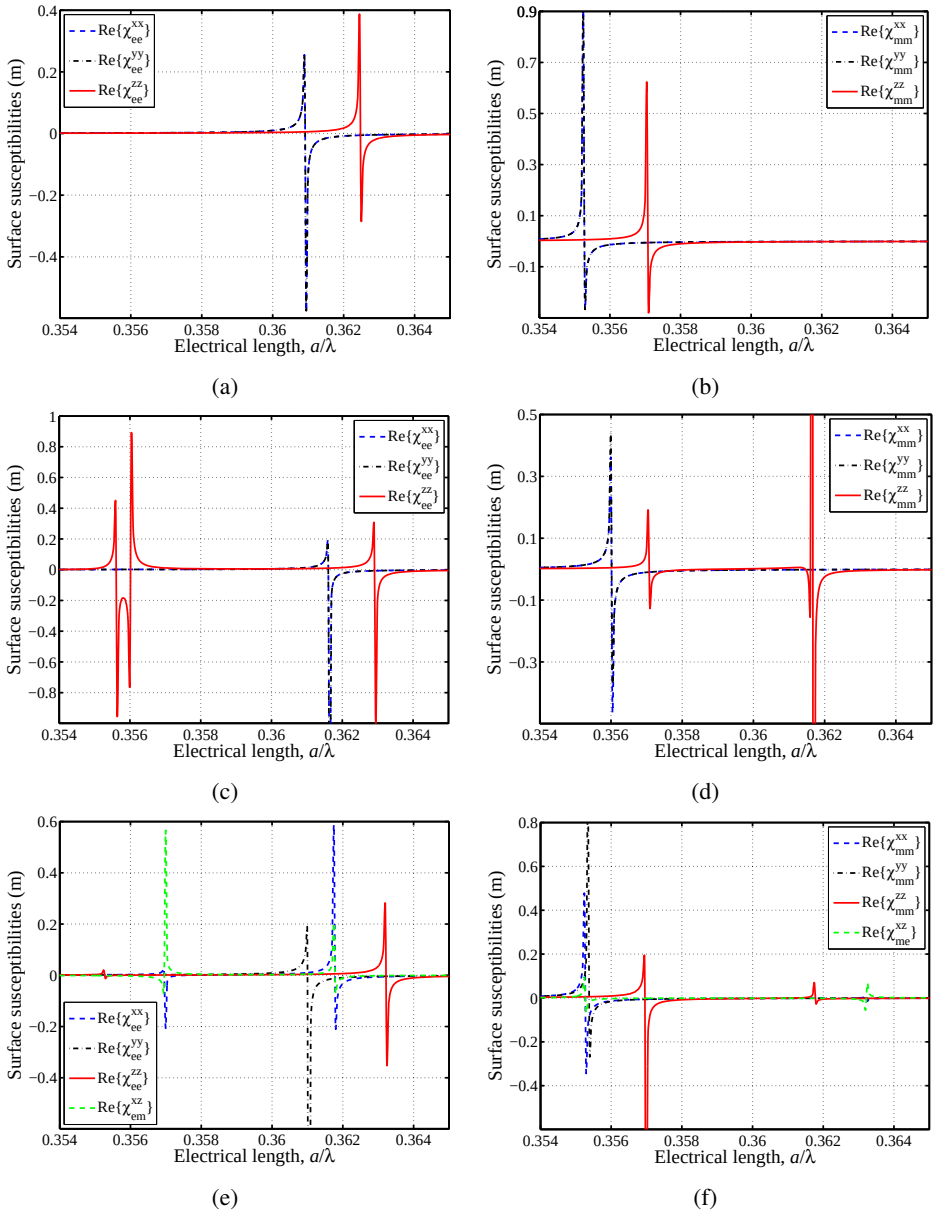

Figure 4: Surface susceptibilities for a lossless metafilm with magneto-dielectric spheres for (a),(b) the K-B method, (c),(d) the H-M method, and (e),(f) the proposed method for $\theta = 75^\circ$.

ly in the zones where the parameters χ_{mm}^{xx} and χ_{ee}^{xx}, respectively, become resonant. These artificial resonances stem from the calculation formulas of these parameters, which explicitly depend on the respective tangential components. These artifacts constitute one of the main drawbacks of the H-M method, as we shall soon discuss.

Regarding the proposed method, since $[\alpha]$ has the form of (14), with $\alpha_{ee}^{xx} = \alpha_{ee}^{yy} = \alpha_{ee}^{zz}$, $\alpha_{mm}^{xx} = \alpha_{mm}^{yy} = \alpha_{mm}^{zz}$ and the metafilm is lossless, the surface susceptibility matrix $[\chi]$ can be calculated from the simplified expression (30) and reads

$$[\chi] = \begin{bmatrix} \chi_{ee}^{xx} & \chi_{ee}^{xy} & 0 & 0 & 0 & \chi_{em}^{xz} \\ \chi_{ee}^{xy} & \chi_{ee}^{yy} & 0 & 0 & 0 & \chi_{em}^{yz} \\ 0 & 0 & \chi_{ee}^{zz} & \chi_{me}^{xz} & \chi_{me}^{yz} & 0 \\ 0 & 0 & \chi_{me}^{xz} & \chi_{mm}^{xx} & \chi_{mm}^{xy} & 0 \\ 0 & 0 & \chi_{me}^{yz} & \chi_{mm}^{xy} & \chi_{mm}^{yy} & 0 \\ \chi_{em}^{xz} & \chi_{em}^{yz} & 0 & 0 & 0 & \chi_{mm}^{zz} \end{bmatrix}. \tag{34}$$

We observe that $[\chi]$ is symmetric and contains 12 different real parameters, which depend on the wavevector of the incident wave. For a wave impinging on the metafilm under an angle $\theta = 75^\circ$, the corresponding parameters are shown in Figs 4(e) and 4(f). Contrary to the other techniques, one may detect that $\chi_{ee}^{xx} \neq \chi_{ee}^{yy}$ and $\chi_{mm}^{xx} \neq \chi_{mm}^{yy}$ in this case. Furthermore, the off-diagonal terms χ_{em}^{xz} and χ_{me}^{xz} are non-zero and, thus, cannot be excluded from the analysis. In addition, due to the absence of bianisotropic effects at the microscopic level, these non-zero terms can be associated with weak spatial dispersion phenomena (lattice dispersion). Similar phenomena have been reported in the literature for 3-D periodic structures of non-bianisotropic scatterers [Fietz and Shvets (2010); Alù (2011)].

To highlight the importance of these off-diagonal terms, we will, now, compare the efficiency of the three aforementioned models in the prediction of the reflection and transmission coefficients of the metafilm. Therefore, taking into account the form of $[\chi]$ in (34) and inserting it into (13), the reflection and transmission coefficients for the two possible polarizations are determined by

$$R_\perp = \frac{-j\frac{k_0}{2\cos\theta}\left(A - \chi_{mm}^{yy}\cos^2\theta\right)}{1 - \frac{k_0^2}{4}\chi_{mm}^{yy}A + j\frac{k_0}{2\cos\theta}\left(A + \chi_{mm}^{yy}\cos^2\theta\right)}, \tag{35a}$$

$$T_\perp = \frac{1 + \frac{k_0^2}{4}\chi_{mm}^{yy}A}{1 - \frac{k_0^2}{4}\chi_{mm}^{yy}A + j\frac{k_0}{2\cos\theta}\left(A + \chi_{mm}^{yy}\cos^2\theta\right)}, \tag{35b}$$

$$R_\parallel = \frac{j\frac{k_0}{2\cos\theta}\left(B - \chi_{ee}^{yy}\cos^2\theta\right)}{1 - \frac{k_0^2}{4}\chi_{ee}^{yy}B + j\frac{k_0}{2\cos\theta}\left(B + \chi_{ee}^{yy}\cos^2\theta\right)}, \tag{36a}$$

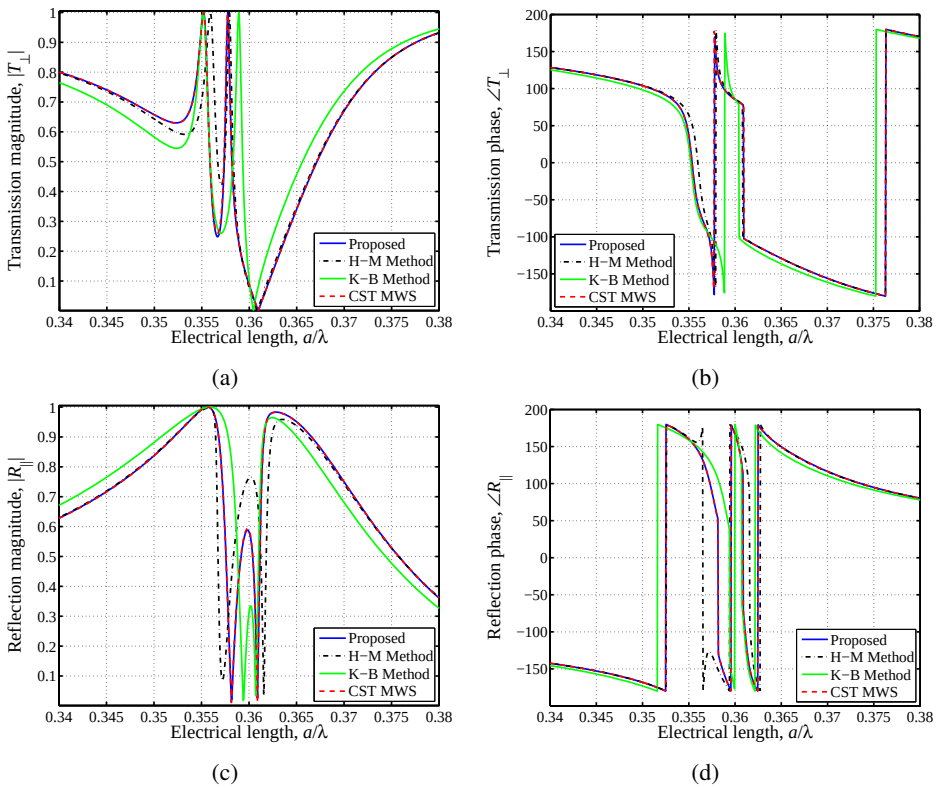

Figure 5: Comparisons of the scattering coefficients predicted from the various models. (a),(b) Magnitude and phase of the transmission coefficients $T_\perp$ and (c),(d) magnitude and phase of the reflection coefficients $R_\parallel$ for $\theta = 75^\circ$.

$$T_\parallel = \frac{1 + \frac{k_0^2}{4}\chi_{ee}^{yy} B}{1 - \frac{k_0^2}{4}\chi_{ee}^{yy} B + j\frac{k_0}{2\cos\theta}\left(B + \chi_{ee}^{yy}\cos^2\theta\right)}, \tag{36b}$$

where $A = \chi_{ee}^{xx} + \chi_{mm}^{zz}\sin^2\theta + 2\chi_{em}^{xz}\sin\theta$ and $B = \chi_{mm}^{xx} + \chi_{ee}^{zz}\sin^2\theta - 2\chi_{me}^{xz}\sin\theta$. Note that χ_{em}^{xz} and χ_{me}^{xz} are included in the expressions for the perpendicular and the parallel polarization, respectively. This observation, together with the susceptibilities of Fig. 4, will help us to better interpret the predictions of the three models.

Next, by considering a $\theta = 75^\circ$ incidence and inserting the surface susceptibilities of Fig. 4 into (35b), we acquire the magnitude (Fig. 5(a)) and phase (Fig. 5(b)) of the transmission coefficient, $T_\perp$, around the first resonance frequency. We first note that, due to the rather large electrical length of the unit cell of the metafilm at this frequency band, the K-B method can approximate only the shape of the simulated scattering coefficients, as a result of its quasistatic approximations. Moreover, fo-

cusing on the specific frequency $a/\lambda = 0.357$ and the susceptibility terms of (35b), we promptly detect that both the K-B and H-M models predict non-zero value only for the χ_{mm}^{zz} parameter. On the other hand, for the proposed approach, χ_{ee}^{xx}, χ_{mm}^{zz}, and χ_{em}^{xz} are all non-zero at that frequency. Thus, taking into account the relative magnitudes of these components in Figs 4(e) and 4(f) and their respective weighting coefficients in the expression of A (1, $\sin^2\theta$, and $2\sin\theta$), it can be deduced that χ_{em}^{xz} is at least equally important as χ_{mm}^{zz}. This differentiation of the proposed approach, compared to the K-B and H-M methods, justifies its superior predictive performance in this particular frequency band.

For the same angle of incidence, from (36a), one derives the magnitude (Fig. 5(c)) and phase (Fig. 5(d)) of the reflection coefficient, $R_{\|}$. Contrary to the previous case, χ_{me}^{xz} is non-zero at the $a/\lambda = 0.355$ frequency, yet all methods successfully predict the performance of the metafilm at this point. Thus it is concluded that, in this case, χ_{mm}^{xx} is the dominant term in (36a) and the effect of the off-diagonal term is insignificant. However, the K-B method again departs from the simulation curves in the rest of the spectrum under study, as explained in the previous paragraph. Finally, it should be stressed that the divergence of the H-M approach from the simulation data for $a/\lambda > 0.356$ occurs due to the second, non-physical resonance of χ_{ee}^{zz}, which can be attributed to the sensitivity of its calculation formula (20c) to the noise of the numerical input data.

4.1.2 Lossy case

Let us now assume that the magneto-dielectric spheres are made up of a material with constitutive parameters $\varepsilon_r = 13.8(1 - j0.002)$ and $\mu_r = 11.0(1 - j0.002)$, while all other geometric parameters of the metafilm remain the same as in the previous subsection. The presence of material losses is expected to lead to the occurrence of imaginary parts in the surface susceptibilities for all the models.

In this context, the parameters of the K-B method are shown in Figs 6(a) and 6(b), while those of the H-M method are presented in Figs 6(c) and 6(d)[4]. Evidently, apart from the occurrence of the imaginary parts, the addition of losses leads to more wide and less sharp resonances of surface susceptibilities, compared to the lossless case. For the H-M method, normal components χ_{ee}^{zz} and χ_{mm}^{zz} exhibit again a second, artificial resonance, at the same frequency where the parameters χ_{mm}^{xx} and χ_{ee}^{xx}, correspondingly, become resonant. Moreover, χ_{ee}^{zz} seems to violate the passivity condition around the $a/\lambda = 0.356$ frequency, since its imaginary part becomes positive. This implies that the H-M model is not local at this frequency range and its parameters cannot be treated as characteristic parameters of the structure. On

[4] Parameters χ_{ee}^{yy} and χ_{mm}^{yy} are not included in these figures, since they are again equal to χ_{ee}^{xx} and χ_{mm}^{xx}, respectively, as in the previous case.

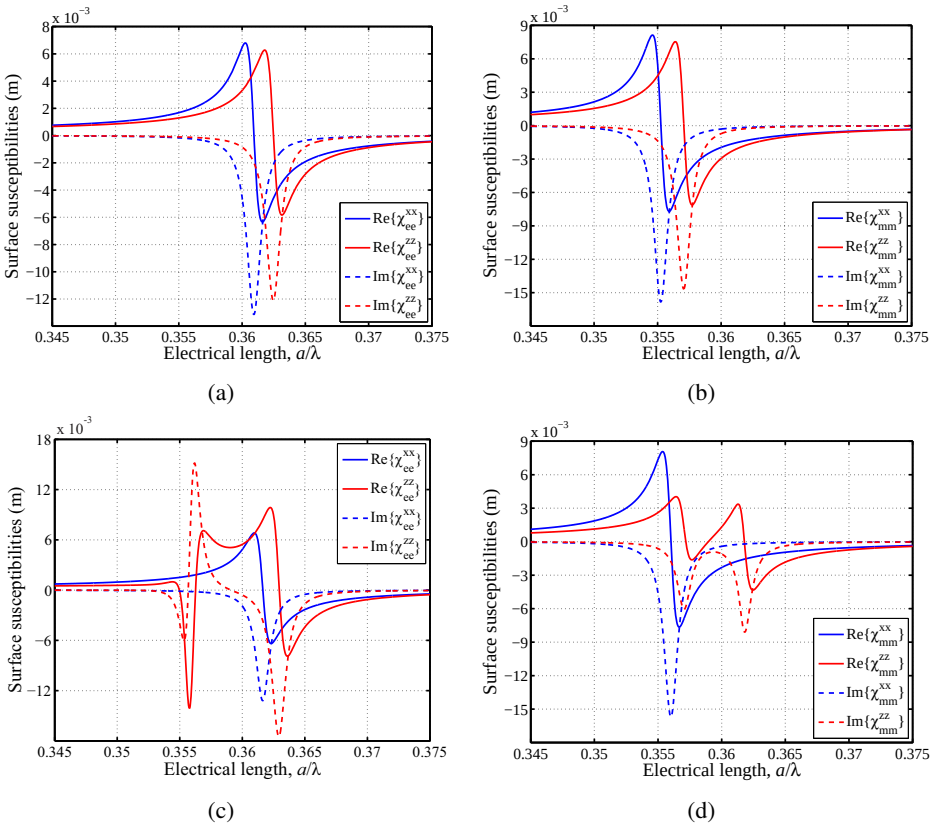

Figure 6: Surface susceptibilities for a lossy metafilm with magneto-dielectric spheres for (a),(b) the K-B method and (c),(d) the H-M method.

the contrary, the surface susceptibilities of the proposed method for $\theta = 45^\circ$ are illustrated in Figs 7(a)-7(c), where only the real parts of the off-diagonal terms take positive values, as anticipated from the non-local nature of the extracted parameters. As a consequence, the latter parameters represent more accurately the physics of the particular problem. Finally, by substituting the surface susceptibilities into (35a), we obtain the magnitude of the reflection coefficient $R_\perp$ of Fig. 7(d). The proposed method is in very good agreement with the CST MWS™ outcomes, apart from a narrow band around $a/\lambda = 0.3555$, where a small fluctuation of χ_{ee}^{xx} leads to a subsequent deviation from the simulation results. This is the region where the H-M method also loses its accuracy, due to the positive values of $\mathrm{Im}\{\chi_{ee}^{zz}\}$, while the K-B method deviates from the other approaches around the resonance band.

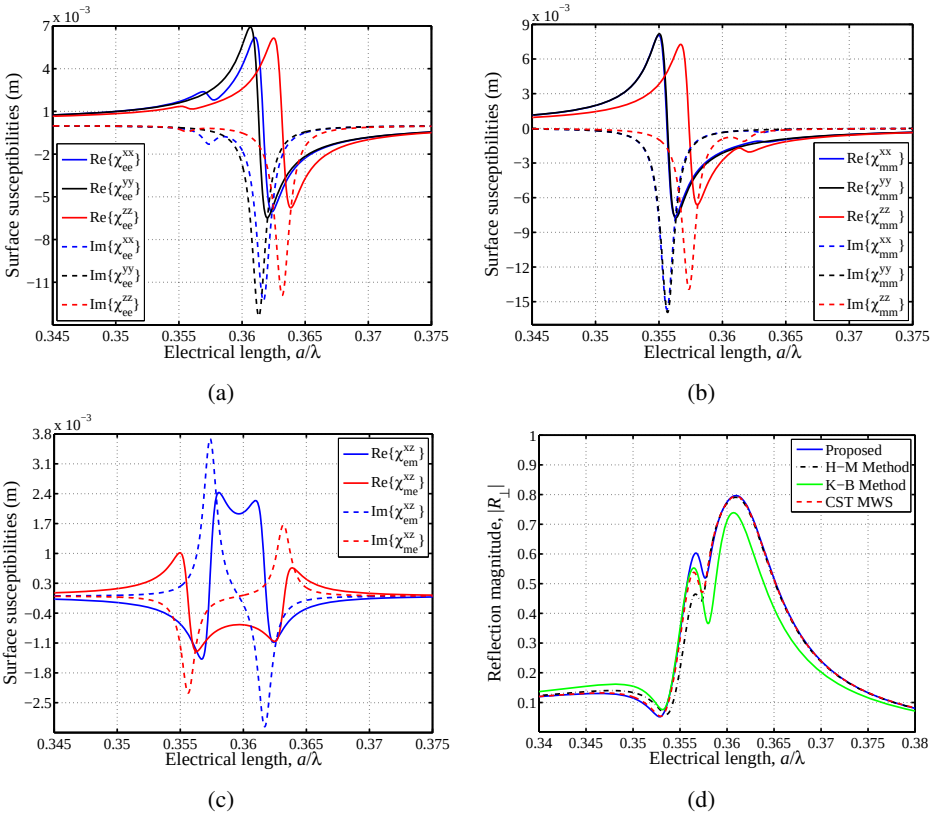

Figure 7: (a),(b),(c) Surface susceptibilities for a lossy metafilm with magneto-dielectric spheres for the proposed method for $\theta = 45^\circ$, and (d) comparison of the magnitude of the reflection coefficients $R_{\parallel}$ of the various models for $\theta = 45^\circ$.

4.2 Microstrip Ω-shaped resonator

4.2.1 Lossless case

Planar metallic scatterers are another attractive solution for the design of practical metafilms, since they can be easily fabricated via standard photolithographic techniques. Here, we will investigate metafilms consisting of the microstrip Ω-shaped resonator of Fig. 8(a). This specific meta-atom has been utilized in the implementation of various realistic devices, like reciprocal microwave phase shifters [Saadoun and Engheta (1994)], DNG materials with low losses [Ran, Huangfu, Chen, Li, Zhang, Chen and Kong (2004); Lheurette, Houzet, Carbonell, Zhang, Vanbesien and Lippens (2008)], waveguide power splitters [Di Palma, Bilotti, Toscano and Vegni (2012)] and antenna radomes [Basiry, Abiri and Yahaghi (2011)]. This par-

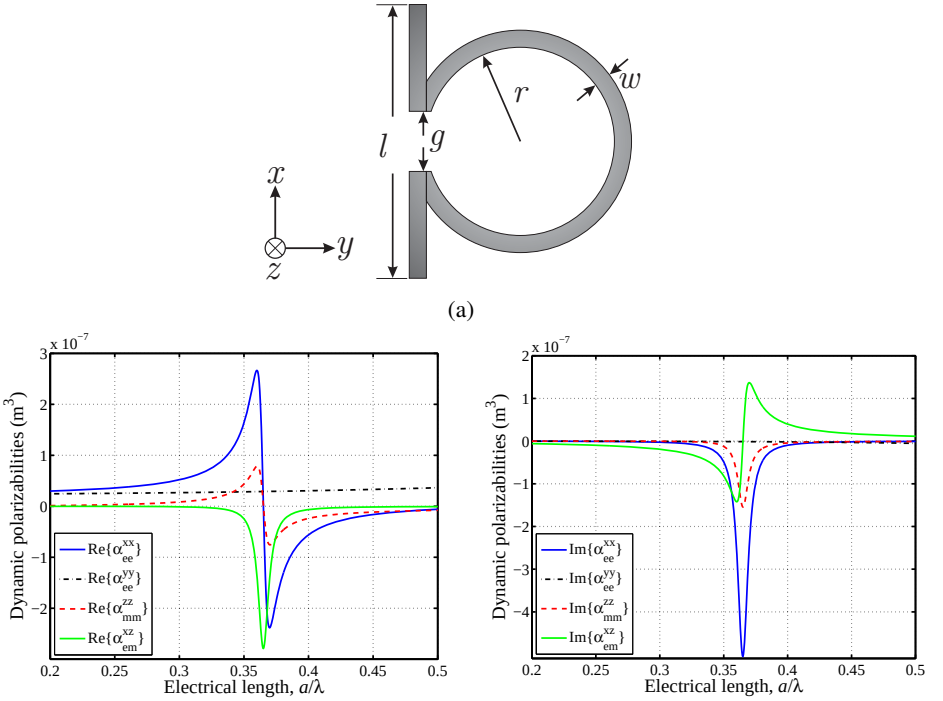

Figure 8: (a) Ω-shaped resonator with dimensions: $l = 3.5\,\text{mm}$, $r = 1.2\,\text{mm}$, $w = 0.3\,\text{mm}$, and $g = 0.2\,\text{mm}$, (b) real, and (c) imaginary part of the dynamic particle polarizabilities derived via [Karamanos, Dimitriadis and Kantartzis (2012)].

ticle can be modeled via an electric dipole moment, p_x, and a magnetic dipole moment, m_z, which are induced when it is excited from an x-directed electric field and/or a z-directed magnetic field. Furthermore, electric charges can also be accumulated along the y-direction, when a y-directed electric field is externally applied. However, the latter polarization is not coupled to the previous ones. To sum up, the polarizability matrix $[\alpha]$ of the Ω particle can be written as

$$[\alpha] = \begin{bmatrix} \alpha_{ee}^{xx} & 0 & \alpha_{em}^{xz} \\ 0 & \alpha_{ee}^{yy} & 0 \\ \alpha_{me}^{zx} & 0 & \alpha_{mm}^{zz} \end{bmatrix}, \tag{37}$$

where, due to the Onsager-Casimir principle, $\alpha_{em}^{xz} = -\alpha_{me}^{zx}$ also holds.

Next, let us concentrate on a metafilm consisting of the doubly periodic repetition of Ω resonators, with the dimensions provided in the caption of Fig. 8(a). Assuming a square unit cell with $a = b = 7.5\,\text{mm}$, the analysis is performed for frequencies $8 <$

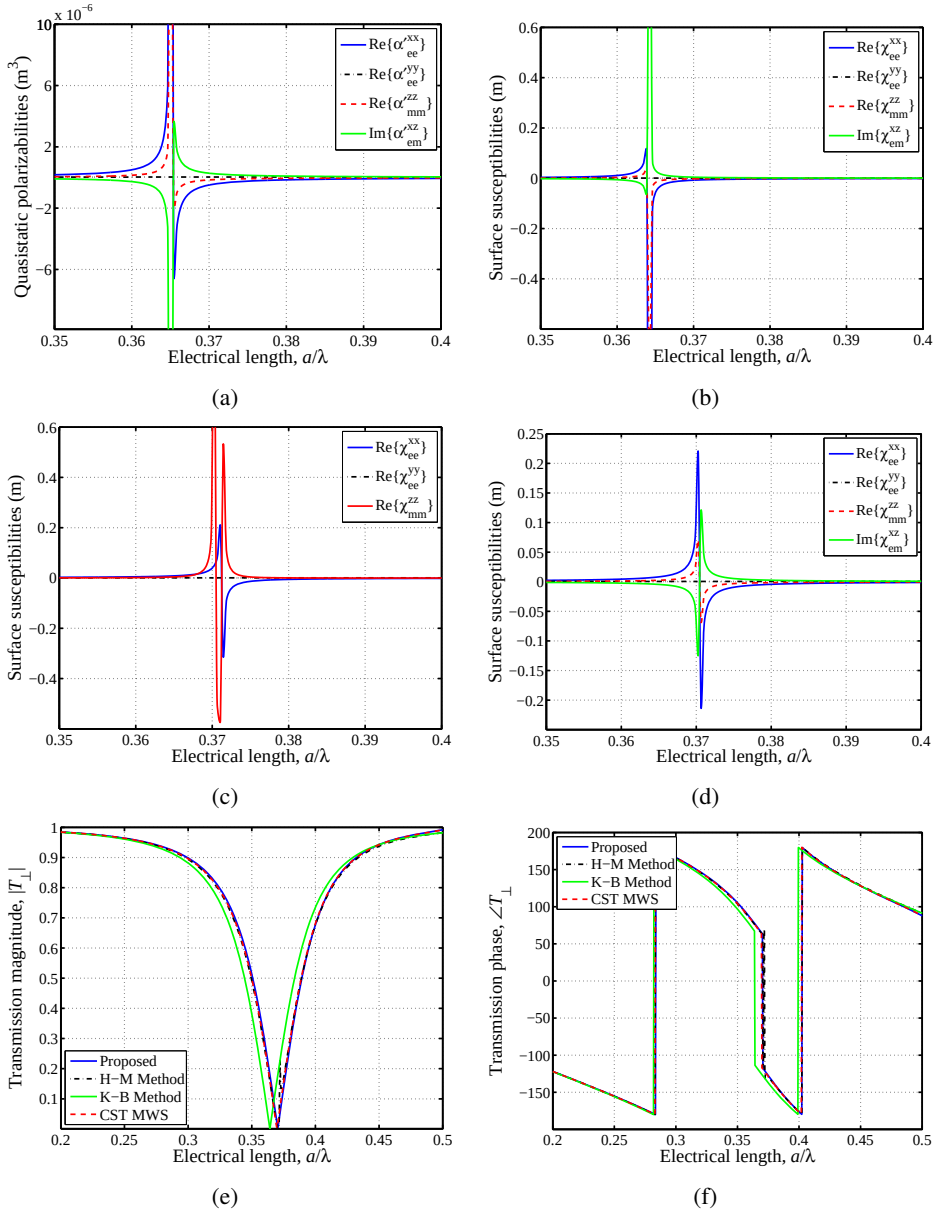

Figure 9: (a) Quasistatic susceptibilities of the lossless Ω-resonator with the dimensions of Fig. 8(a). Surface susceptibilities of the (b) K-M method, (c) H-M method, and (d) proposed method for $\theta = 75^\circ$. (e) Magnitude and (f) phase of the transmission coefficients $T_\perp$ predicted from the various models for $\theta = 75^\circ$.

$f < 20\,\text{GHz}$, which correspond to the electrical length $0.2 < a/\lambda < 0.5$. In these microwave frequencies, metals are known to behave as perfect electric conductors (PEC) and the corresponding dynamic Ω particle polarizabilities need to satisfy the Sipe-Kranendonk conditions of (4). Hence, the application of a properly developed retrieval algorithm [Karamanos, Dimitriadis and Kantartzis (2012)], provides the unkown elements of (37), plotted in Figs 8(b) and 8(c), which comply with the energy conservation requirements. It can be seen that at $a/\lambda = 0.365$ the $\text{Re}\{\alpha_{ee}^{xx}\}$, $\text{Re}\{\alpha_{mm}^{zz}\}$, and $\text{Im}\{\alpha_{em}^{xz}\}$ terms become simultaneously resonant, while $\text{Re}\{\alpha_{ee}^{yy}\}$ is practically constant throughout the considered spectrum. Moreover, $\text{Im}\{\alpha_{ee}^{xx}\}$, $\text{Im}\{\alpha_{mm}^{zz}\}$, and $\text{Re}\{\alpha_{em}^{xz}\}$ are negative, as required from passivity.

In order to apply the K-B method, it is necessary to determine the quasistatic polarizabilities of the scatterer. The latter can be directly obtained via the procedure described in [Yatsenko, Maslovski, Tretyakov, Prosvirnin and Zouhdi (2003)] and are given in Fig. 9(a). We detect that by "removing" the radiation losses from the dynamic polarizabilities, the resonances in the corresponding quasistatic terms become narrower and sharper. Then, the $[\chi]$ matrix of the K-B method, which has a similar form to the $[\alpha]$ matrix of (37), can be calculated. These susceptibilities, obtained via (16), are shown in Fig. 9(b) and are similar in shape with the corresponding quasistatic polarizability terms. In contrast, the parameters of the H-M, which are depicted in Fig. 9(c), lead to some very interesting conclusions. Specifically, since this model includes only diagonal terms of the $[\chi]$ matrix, the magnetoelectric coupling of the metafilm is improperly incorporated into χ_{mm}^{zz}, leading to a second, non-physical resonance of this parameter. However, this inconsistency is to be expected, since the H-M method has $-$ for the moment $-$ been developed only for metafilms with non-bianisotropic scatterers. Lastly, for the proposed technique, $[\chi]$ takes the general form of (32) and is an Hermitian matrix, due to the absence of losses. This means that only 6 of the $[\chi]$ matrix parameters are independent, due to the symmetries that arise from the Hermitian property $\chi_{em}^{xz} = \overset{*}{\chi}_{me}^{zx}$, $\chi_{em}^{yz} = \overset{*}{\chi}_{me}^{zy}$, and $\chi_{ee}^{xy} = \overset{*}{\chi}_{ee}^{yx}$. Utilizing (29) for $\theta = 75^\circ$, we derive the susceptibilities of Fig. 9(d), which look similar in shape to the respective dynamic polarizability terms, but shifted toward slightly higher frequencies. This shift may be attributed to the dynamic interactions between the scatterers in the array. However, due to the presence of strong bianisotropic effects at the particle level, off-diagonal terms, other than χ_{em}^{xz} and χ_{me}^{zx}, are practically negligible and do not affect the behavior of the structure.

For a direct comparison of the methods, under study, we insert (32) into (13) and, similarly to the previous section, closed-form expressions are determined for the

reflection and transmission coefficients of the two linear eigen-polarizations

$$R_{\perp} = \frac{-j\frac{k_0}{2\cos\theta}\left(\chi_{ee}^{xx} + \chi_{mm}^{zz}\sin^2\theta + \chi_{em}^{xz}\sin\theta + \chi_{me}^{zx}\sin\theta\right)}{1 + j\frac{k_0}{2\cos\theta}\left(\chi_{ee}^{xx} + \chi_{mm}^{zz}\sin^2\theta + \chi_{em}^{xz}\sin\theta + \chi_{me}^{zx}\sin\theta\right)}, \tag{38a}$$

$$T_{\perp} = \left[1 + j\frac{k_0}{2\cos\theta}\left(\chi_{ee}^{xx} + \chi_{mm}^{zz}\sin^2\theta + \chi_{em}^{xz}\sin\theta + \chi_{me}^{zx}\sin\theta\right)\right]^{-1}, \tag{38b}$$

$$R_{\parallel} = \frac{-j\frac{k_0}{2}\chi_{ee}^{yy}\cos\theta}{1 + j\frac{k_0}{2}\chi_{ee}^{yy}\cos\theta}, \tag{39a}$$

$$T_{\parallel} = \left[1 + j\frac{k_0}{2}\chi_{ee}^{yy}\cos\theta\right]^{-1}, \tag{39b}$$

for which the relations $1 + R_{\perp} = T_{\perp}$ and $1 + R_{\parallel} = T_{\parallel}$ hold. Prior to the comparison of the different models, some general comments can be made regarding the above expressions. First, for the case of lossless scatterers, the Hermitian property leads to the following simplification $\chi_{em}^{xz}\sin\theta + \chi_{me}^{zx}\sin\theta = 2\mathrm{Re}\{\chi_{em}^{xz}\}\sin\theta$. Nevertheless, since the real part of χ_{em}^{xz} was found to be negligible in Fig. 9(d), the reflection and transmission properties for the perpendicular polarization, calculated via (38), are mainly determined by the real parts of the diagonal susceptibility terms. Likewise, the scattering properties of the metafilm illuminated by a plane wave with parallel polarization depends solely on the term χ_{ee}^{yy}, which was found to be practically constant in all the models (Figs 9(b)-9(d)).

Proceeding to the explicit comparison of the various techniques for a plane wave with perpendicular polarization and incidence angle $\theta = 75^{\circ}$, from (38b) we obtain the magnitude and phase of the transmission coefficient, $T_{\perp}$, which are depicted in Figs 9(e) and 9(f), respectively. The proposed algorithm appears to be in excellent agreement with the simulation results throughout the examined frequency range. The same applies to the outcomes of the H-M method, with the exception of a narrow interval around $a/\lambda = 0.372$, where a small transmission peak arises. The location of this peak matches perfectly with that of the aforementioned non-physical resonance of χ_{mm}^{zz} (Fig. 9(c)), which is the result of a numerical defect. Finally, the K-B method correctly reproduces the simulation results, but only with a small frequency downshift. This phenomenon is a common occurrence in this approach, when the electrical length of the unit cell is higher than approximately $a/\lambda > 0.15$. In such cases, the retardation effects from the propagation of the microscopic scattered fields (namely, the fields which are scattered by each meta-atom of the array) along the lattice tend to be significant for the performance of the structure. These effects, which are not taken into account by the K-B method (but are properly incorporated into the elements of $[C]$ in our approach) are, in fact, the reason for the appearance of the weak spatial dispersion effects mentioned before.

4.2.2 Lossy case

To examine the performance of a lossy structure with planar metallic scatterers, we simply downscale the dimensions of the unit cell and the resonators by two orders of magnitude (i.e. $l = 35\,\mu$m, $r = 12\,\mu$m, $w = 3\,\mu$m, $g = 2\,\mu$m, and $a = b = 75\,\mu$m, with reference to Fig. 8(a)). The frequency range of our study is, similarly, upscaled and becomes $0.8 < f < 2$ THz, which again corresponds to an electrical length of the unit cell $0.2 < a/\lambda < 0.5$. At these frequencies, metals cannot be treated as perfect conductors and they exhibit ohmic losses which are increasing with frequency, owing to their plasmonic behavior [Maier (2007)].

By repeating the steps of the prior subsection, we initially acquire the polarizabilities of Figs 10(a) and 10(b). The latter are qualitatively similar to those of the lossless case, yet are several orders of magnitude smaller, since − in principle − the magnitude of the polarizabilities is comparable to the scatterer volume. Furthermore, due to the presence of losses, the resonances are less accentuated than those of the lossless case. Then, these polarizabilities are employed for the implementation of the K-B method, leading to the susceptibilities of Figs 10(c) and 10(d). These parameters are found to be practically identical to the surface averages of the polarizabilities, namely $\chi_{ee}^{xx} = \alpha_{ee}^{\prime xx}/(ab)$, $\chi_{ee}^{yy} = \alpha_{ee}^{\prime yy}/(ab)$, $\chi_{mm}^{zz} = \alpha_{mm}^{\prime zz}/(ab)$, and $\chi_{em}^{xz} = \alpha_{em}^{\prime xz}/(ab)$. This is an indication that the interactions between the scatterers are considered to be rather weak, compared to the individual particle resonances. Conversely, the proposed method for $\theta = 75^\circ$ leads to the surface parameters of Figs 10(e) and 10(f). Despite their optical similarity to the K-B susceptibilities, these parameters are, in fact, totally different, as the dynamic particle interactions are properly incorporated via the interaction coefficient matrix $[C]$.

At this point, it is particularly instructive to study the extracted surface susceptibilities of the H-M method, presented in Figs 11(a) and 11(b). One observes that, whereas χ_{ee}^{xx} appears to be in very good agreement with the corresponding parameters of the other models, this does not apply to χ_{mm}^{zz}. Specifically, $\mathrm{Re}\{\chi_{mm}^{zz}\}$ exhibits a distorted resonance, while $\mathrm{Im}\{\chi_{mm}^{zz}\}$ takes positive values in the region just above the resonance, thus violating the passivity condition and breaking the local nature of the model.

In order to further highlight the fact that χ_{mm}^{zz} is not a characteristic parameter of the structure at this frequency band, we plot its real (Fig. 11(c)) and imaginary (Fig. 11(d)) parts, as extracted for different choices of the input parameter θ in (20d). Both the real and imaginary part are found to strongly depend on angle θ, thus verifying that (20d) does not determine a unique characteristic parameter of the metafilm. Furthermore, by comparing (38) with (18), we can claim that the actual parameter retrieved from the H-M method is, in this case, the sum $\hat{\chi}_{mm}^{zz} = \chi_{mm}^{zz} +$

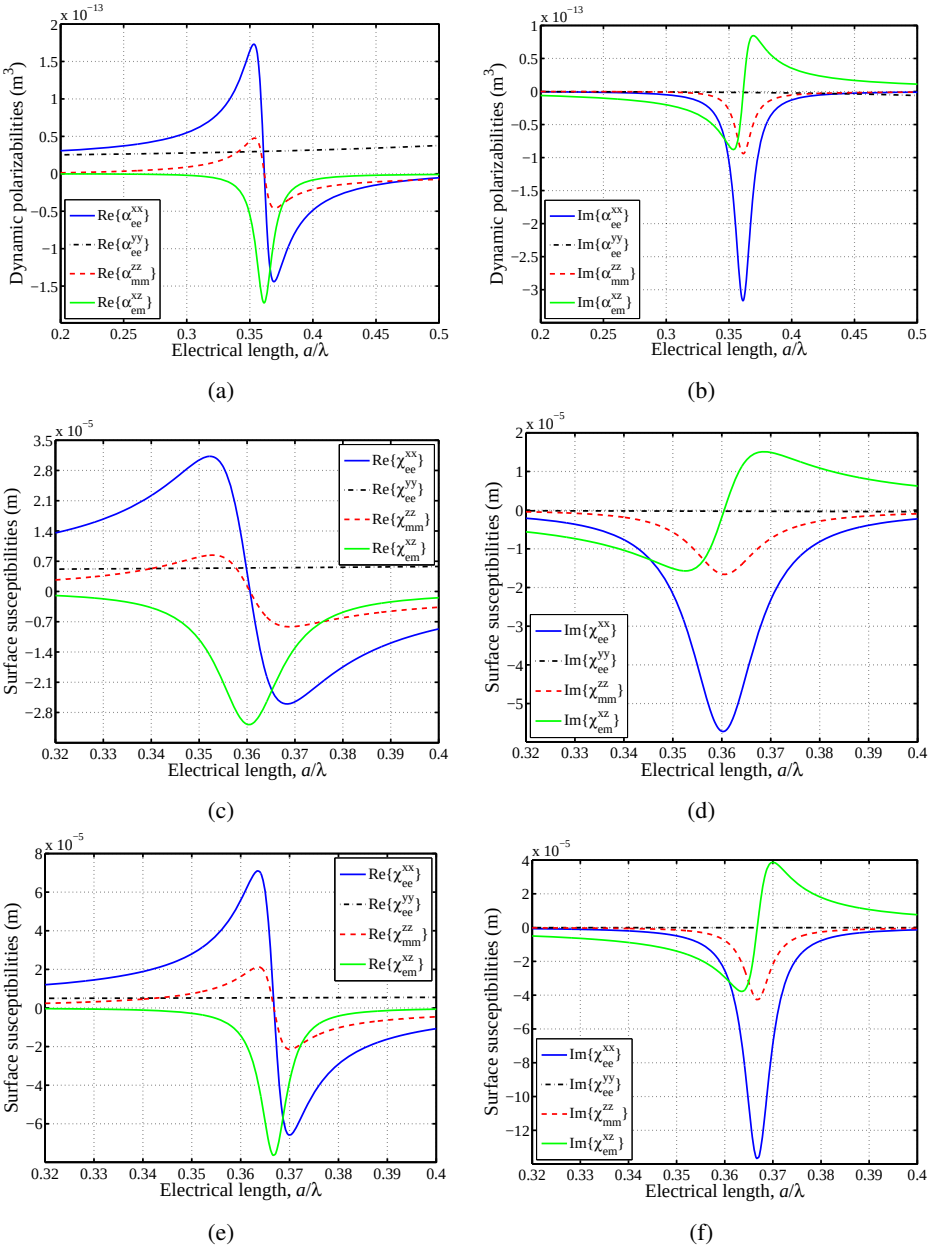

Figure 10: (a) Real and (b) imaginary parts of the dynamic polarizabilities for the lossy (downscaled) Ω-resonator. Surface susceptibilities of (c),(d) the K-B method and (e),(f) the proposed method for $\theta = 75°$.

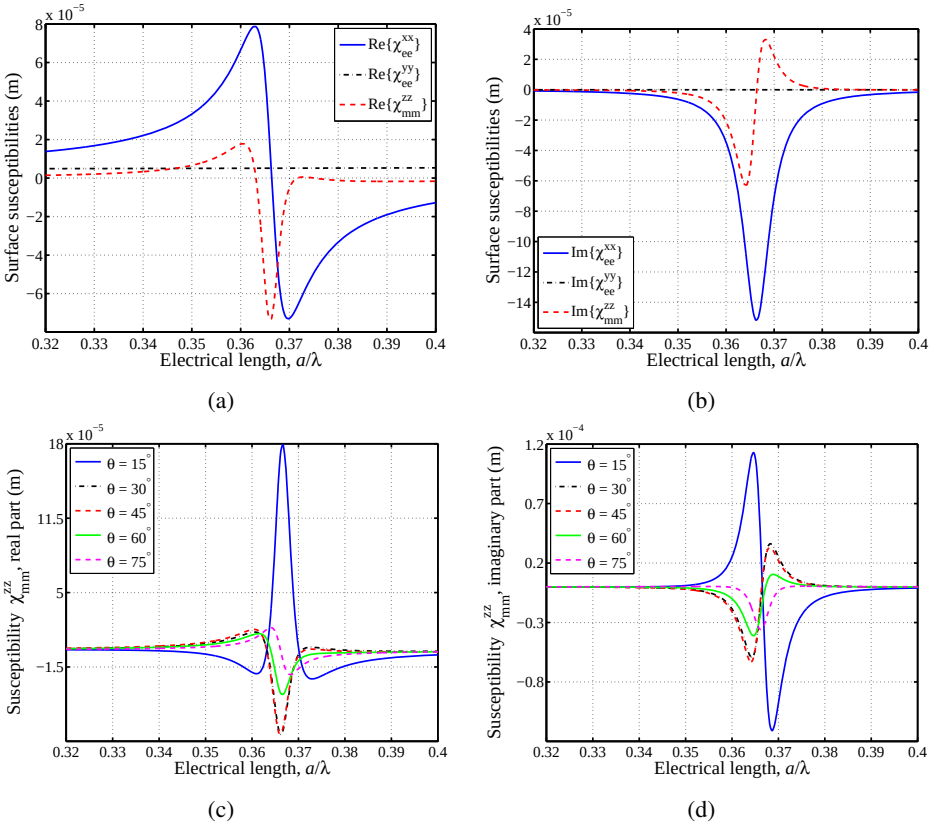

Figure 11: Surface susceptibilities of the H-M method derived from (20) (a),(b) for $\theta = 45^\circ$ and (c),(d) real and imaginary parts of χ_{mm}^{zz} for various values of angle θ.

$(\chi_{em}^{xz} + \chi_{me}^{zx})/\sin\theta$ and not the local parameter χ_{mm}^{zz} itself. Hence, an appropriate extension of the H-M algorithm for bianosotropic metafilms is necessary to retrieve physically-meaningful (characteristic) parameters.

Finally, by utilizing (38b) we acquire the transmission coefficient of the perpendicular polarization, $T_\perp$, for an incident wave with $\theta = 75^\circ$, as shown in Figs 12(a) and 12(b) (magnitude and phase, respectively). First of all, one may note the perfect matching of the reference CST MWS™ simulation results with the predictions of our model, throughout the examined spectrum. However, the H-M method is also in almost perfect agreement with the these results, since the non-locality of χ_{mm}^{zz} and the loss of its physical meaning does not deprive the method of its applicability, even in this case. Regarding the K-B algorithm, it is deemed unsatisfactory around the resonance region as, apart from the expected frequency downshift, it fails to accurately predict the magnitude and the phase of the transmission coeffi-

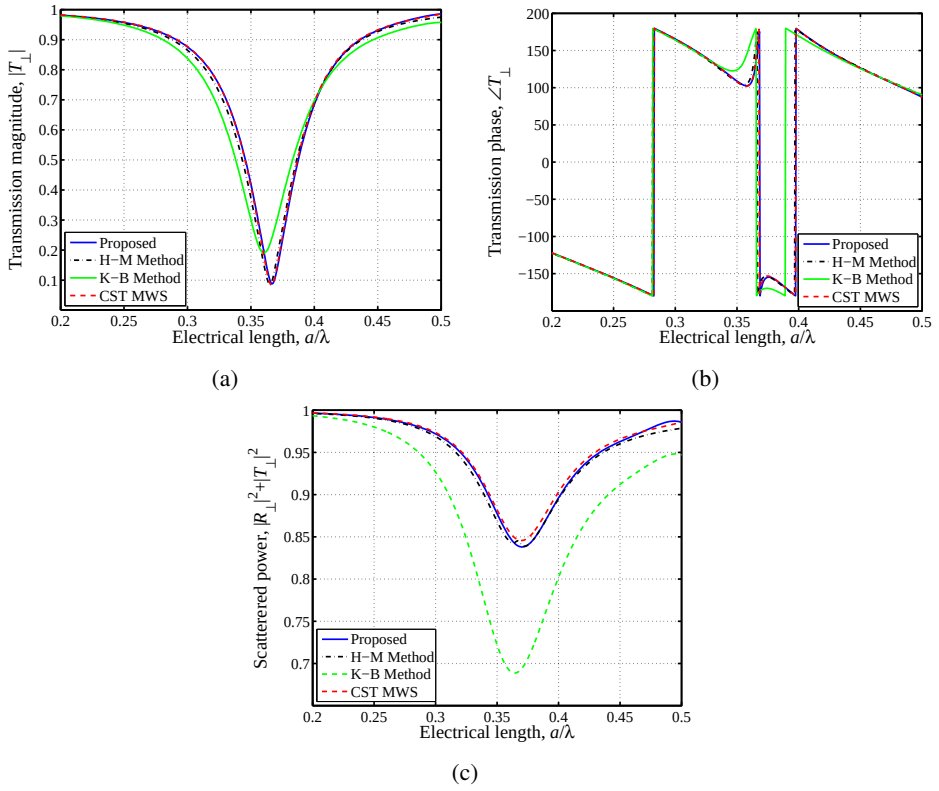

Figure 12: (a) Magnitude, (b) phase of the transmission coefficient $T_\perp$, and (c) total scattered power $|R_\perp|^2+|T_\perp|^2$ for $\theta = 75^\circ$, as predicted from the various models.

cient. This is, also, manifested in the plot of the total scattered power, $|R_\perp|^2+|T_\perp|^2$, of Fig. 12(c), where the K-B method is shown to significantly overestimate the resonance losses, compared to the other techniques.

5 Conclusions

In this paper, we have comprehensively examined the three main general-purpose surface susceptiblity models existing in the literature, which have been developed withing the realm of the dipole approximation technique. Via exhaustive comparisons, both for lossless and lossy metafilms of magneto-dielectric spheres and microstrip Ω-shaped resonator, we have managed to trace the main assets and limitations of these methods. Specifically, it has been found that the K-B method, based on the assumption of quasistatic particle interactions, is the least accurate approach. This can be attributed to the size of the typical meta-atoms as well as to

their dense packing in realistic metafilms. Hence, the interactions between the scatterers are usually strong and depend on the excitation method, while the resulting weak spatial dispersion phenomena, potentially important for the proper prediction of the metafilm's scattering properties, are totally ignored from this approach. On the other hand, the H-M method is proven very reliable and accurate, despite some defects that frequently occur, due to the sensitivity of its retrieval formulas on the noise of its input parameters (simulated reflection and transmission coefficients). However, its extracted parameters may lose their physical meaning in some cases, even in the absence of bianisotropic effects at the particle level. Finally, the proposed non-local procedure is found to be the most accurate in all cases, but it comes with a cost of a higher number of surface susceptibilities and, thus, with a higher implementation complexity. However, this drawback is counterbalanced from the proper incorporation of the spatial dispersion phenomena of the metafilms.

Acknowledgement: This research has been co-financed by the European Union (European Social Fund − ESF) and Greek national funds through the Operational Program "Education and Lifelong Learning" of the National Strategic Reference Framework (NSRF) − Research Funding Program: Aristeia. Investing in knowledge society through the European Social Fund.

References

Alù, A. (2011): First-principles homogenization theory for periodic metamaterials. *Phys. Rev. B*, vol. 84, no. 7, pp. 075153(1–18).

Basiry, R.; Abiri, H.; Yahaghi, A. (2011): Electromagnetic performance analysis of omega-type metamaterial radomes. *Int. J. RF and Microw. CAD Engr.*, vol. 21, no. 6, pp. 665–673.

Belokopytov, G. V.; Zhuravlev, A. V.; Terekhov, Y. E. (2011): Transmission of an electromagnetic wave through a bianisotropic metafilm. *Physics of Wave Phenomena*, vol. 19, no. 4, pp. 280–286.

Belov, P. A.; Maslovski, S. I.; Simovski, K. R.; Tretyakov, S. A. (2003): A condition imposed on the electromagnetic polarizability of a bianisotropic lossless scatterer. *Technical Phys. Lett.*, vol. 29, no. 9, pp. 718–720.

Belov, P. A.; Simovski, C. R. (2005): Homogenization of electromagnetic crystals formed by uniaxial resonant scatterers. *Phys. Rev. E*, vol. 72, no. 2, pp. 1–15.

Bhattacharyya, A. K. (2014): Accuracy of Floquet model in predicting performances of finite arrays. *IEEE Antennas Wireless Propag. Lett.*, vol. 13, pp. 19–22.

Collin, R. E. (1991): *Field Theory of Guided Waves*. IEEE Press, Piscataway.

CST MWS™ (2012): *Computer Simulation Technology: Microwave Studio*.

Di Palma, L.; Bilotti, F.; Toscano, A.; Vegni, L. (2012): Design of a waveguide power splitter based on the employment of bi-omega resonators. *Microw. Opt. Technol. Lett.*, vol. 54, no. 9, pp. 2091–2095.

Dimitriadis, A. I.; Kantartzis, N. V.; Tsiboukis, T. D. (2013): Consistent modeling of periodic metasurfaces with bianisotropic scatterers for oblique TE-polarized plane wave excitation. *IEEE Trans. Magn.*, vol. 49, no. 5, pp. 1769–1772.

Dimitriadis, A. I.; Sounas, D. L.; Kantartzis, N. V.; Caloz, C.; Tsiboukis, T. D. (2012): Surface susceptibility bianisotropic matrix model for periodic metasurfaces of uniaxially mono-anisotropic scatterers under oblique TE-wave incidence. *IEEE Trans. Antennas Propag.*, vol. 60, no. 12, pp. 5753–5767.

Fietz, C.; Shvets, G. (2010): Homogenization theory for simple metamaterials modeled as one-dimensional arrays of thin polarizable sheets. *Phys. Rev. B*, vol. 82, no. 20, pp. 205128(1–12).

Holloway, C. L.; Dienstfrey, A.; Kuester, E. F.; O'Hara, J. F.; Azad, A. K.; Taylor, A. J. (2009): A discussion on the interpretation and characterization of metafilms/metasurfaces: The two-dimensional equivalent of metamaterials. *Metamaterials*, vol. 3, no. 2, pp. 100–112.

Holloway, C. L.; Kabos, P.; Mohamed, M. A.; Kuester, E. F.; Gordon, J. A.; Janezic, M. D.; Baker-Jarvis, J. (2010): Realisation of a controllable metafilm/metasurface composed of resonant magnetodielectric particles: measurements and theory. *IET Microw. Antennas Propag.*, vol. 4, no. 8, pp. 1111–1122.

Holloway, C. L.; Kuester, E. F.; Baker-Jarvis, J.; Kabos, P. (2003): A double negative (DNG) composite medium composed of magnetodielectric spherical particles embedded in a matrix. *IEEE Trans. Antennas Propag.*, vol. 51, no. 10, pp. 2596–2603.

Holloway, C. L.; Mohamed, M. A.; Kuester, E. F.; Dienstfrey, A. (2005): Reflection and transmission properties of a metafilm: With an application to a controllable surface composed of resonant particles. *IEEE Trans. Electomagn. Compat.*, vol. 47, no. 4, pp. 853–865.

Idemen, M. (1988): Straightforward derivation of boundary conditions on sheet simulating an anisotropic thin layer. *Electron. Lett.*, vol. 24, no. 11, pp. 663–665.

Karamanos, T. D.; Dimitriadis, A. I.; Kantartzis, N. V. (2012): Polarizability matrix extraction of a bianisotropic metamaterial from the scattering parameters of normally incident plane waves. *Adv. Electromagn.*, vol. 1, no. 3, pp. 64–70.

Koledintseva, M. Y.; Huang, J.; Drewniak, J. L.; DuBroff, R. E.; Archambeault, B. (2012): Modeling of metasheets embedded in dielectric layers. *Progress in Electromagnetics Research B*, vol. 44, pp. 89–116.

Kuester, E. F.; Mohamed, M. A.; Piket-May, M.; Holloway, C. L. (2003): Averaged transition conditions for electromagnetic fields at a metafilm. *IEEE Trans. Antennas Propag.*, vol. 51, no. 10, pp. 2641–2651.

Lheurette, É.; Houzet, G.; Carbonell, J.; Zhang, F.; Vanbesien, O.; Lippens, D. (2008): Omega-type balanced composite negative refractive index materials. *IEEE Trans. Antennas Propag.*, vol. 56, no. 11, pp. 3462–3469.

Maier, S. A. (2007): *Plasmonics: Fundamentals and Applications*. Springer Verlag.

Marqués, R.; Martín, F.; Sorolla, M. (2008): *Metamaterials with Negative Parameter: Theory, Design, and Microwave Applications*. Wiley-Interscience, Hoboken.

Morits, D.; Simovski, C. (2010): Electromagnetic characterization of planar and bulk metamaterials: A theoretical study. *Phys. Rev. B*, vol. 82, no. 16, pp. 165114(1–10).

Raab, R. E.; De Lange, O. L. (2005): *Multipole Theory in Electromagnetism*. Oxford University Press.

Ran, L.; Huangfu, J.; Chen, H.; Li, Y.; Zhang, X.; Chen, K.; Kong, J. A. (2004): Microwave solid-state left-handed material with a broad bandwidth and an ultralow loss. *Phys. Rev. B*, vol. 70, no. 7, pp. 073102(1–3).

Saadoun, M. M. I.; Engheta, N. (1994): Theoretical study of electromagnetic properties of non-local Ω media. *Progress in Electromagnetics Research*, vol. 9, pp. 351–397.

Scher, A. D. (2008): *Boundary effects in the electromagnetic response of a metamaterial using the point-dipole interaction model*. PhD thesis, University of Colorado at Boulder, 2008.

Serdyukov, A.; Semchenko, I.; Tretyakov, S.; Sihvola, A. (2001): *Electromagnetics of Bi-anisotropic Materials: Theory and Applications*. Gordon and Breach, Amsterdam.

Seršić, I.; Tuambilangana, C.; Kampfrath, T.; Koenderink, A. F. (2011): Magnetoelectric point scattering theory for metamaterial scatterers. *Phys. Rev. B*, vol. 83, no. 24, pp. 245102(1–12).

Shore, R. A.; Yaghjian, A. D. (2007): Traveling waves on two-and three-dimensional periodic arrays of lossless scatterers. *Radio Sci.*, vol. 42, no. 6, pp. 1–40.

Sihvola, A. H. (1999): *Electromagnetic Mixing Formulas and Applications*. IEEE, Padstow.

Simovski, C. R.; Tretyakov, S. A. (2007): Local constitutive parameters of metamaterials from an effective-medium perspective. *Phys. Rev. B*, vol. 75, no. 19, pp. 195111(1–10).

Tretyakov, S. A. (2003): *Analytical Modeling in Applied Electromagnetics*. Artech House, Norwood.

Yatsenko, V. V.; Maslovski, S. I.; Tretyakov, S. A.; Prosvirnin, S. L.; Zouhdi, S. (2003): Plane-wave reflection from double arrays of small magnetoelectric scatterers. *IEEE Trans. Antennas Propag.*, vol. 51, no. 1, pp. 2–11.